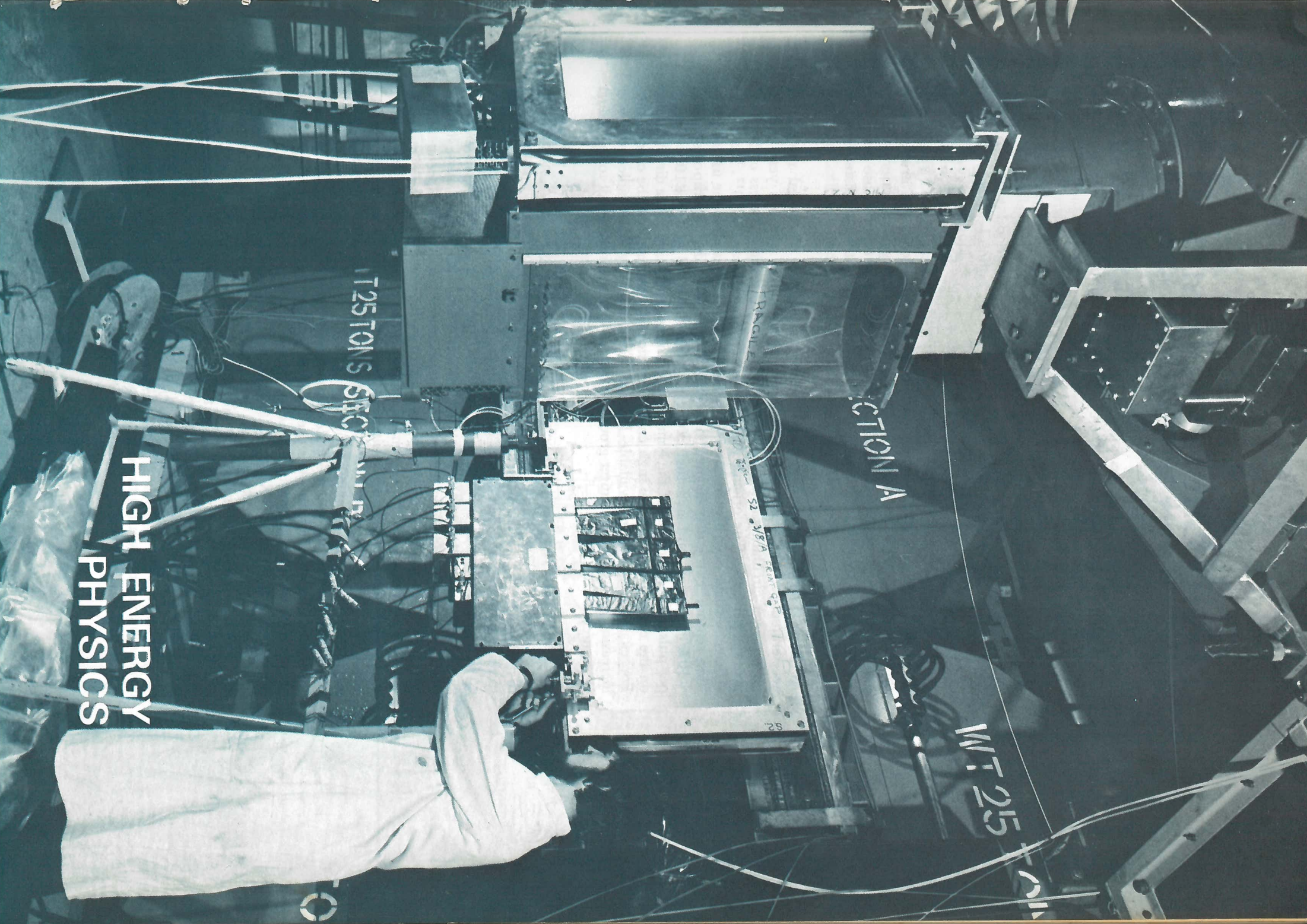
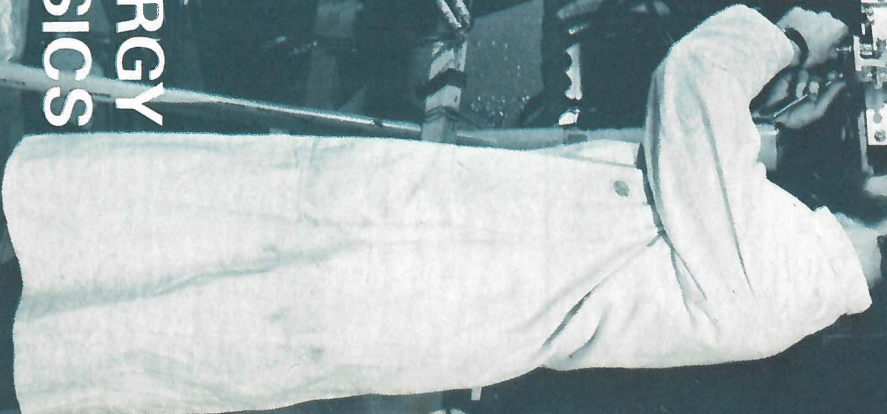


View of the hydrogen target, particle detectors and spectrometer magnet used in Experiment 8.

HIGH ENERGY PHYSICS



High Energy Physics

The year 1970 saw a continuing high level of utilisation of Nimrod, and an increase in the involvement of the Rutherford High Energy Laboratory (RHEL) supported groups at CERN. The universities and institutions whose researches are supported by the facilities of the Rutherford Laboratory are listed in Table 1.

At Nimrod several new records have been established. The total number of accelerated protons was some 20% higher than in any previous year and the highest ever circulating beam intensity was achieved, being in excess of 3×10^{12} protons per pulse. The original design figure for Nimrod was 1×10^{12} . Extraction efficiencies have been higher than ever before; in the X3 beamline the use of a new 'thin septum' extraction magnet, in conjunction with 'header quadrupoles', led to $\sim 40\%$ extraction, and an actual extracted beam down X3 of 1.2×10^{12} protons per pulse. The successes of the Nimrod operations group have had a direct impact on the ease with which the high energy physics programme could be carried out. For example, the large available Nimrod beam intensity has enabled the ever increasing demands by counter groups to be met with minimal delay to individual experiments.

Experiments at Nimrod

During the year, five counter experiments and four bubble chamber experiments were brought to completion. These experiments are all reported in this issue. The first stage in the development of the new experimental hall (Hall 3) reached fruition with two experiments taking data (Experiments 8 & 16). Both are of considerable interest; the first (Experiment 8) studies K^+p interactions and will give information on possible Z^* states (baryon resonances with positive strangeness) which are forbidden in the simple quark model; the second experiment will test for the existence of a charge asymmetry in the eta decay ($\eta^0 \rightarrow \pi^+ \pi^- \pi^0$). A precise experiment by a Columbia group, with 36,000 events, showed an asymmetry which is taken to imply an important symmetry failure in the electromagnetic interaction. The early running of the RHEL experiment has already produced about twice the number of events of the Columbia experiment, so that a significant preliminary result should be obtained before the full data taking is completed. Plans to expand the use of Experimental Hall 3 were completed in early 1970, and installation of the new equipment was started during a six week summer shutdown of the X3 extracted beam. The phase II plans are shown in figure 1. The extracted proton beam will pass through the first target in which interactions produce secondary π 's and K 's for the two existing beamlines ($\pi 8$ and $K15$), and will be refocused on to the new target at the second target station. This target will supply two new beamlines, one of which will be a high momentum pion beam ($\pi 9$) which will be installed in the spring of 1971. When phase II is completed, four out of the nine counter teams using Nimrod will run their experiments simultaneously using the same extracted protons, thus adding further to the operational efficiency of the Nimrod experimental programme.

Table 1

Institutions Participating in the High Energy Physics Programme	
Counter Experiments	Bubble Chamber Experiments
AERE, Harwell	University of Birmingham
University of Bergen, Norway	University of Brussels, Belgium
University of Birmingham	University of Cambridge
University of Bristol	CEN, Saclay
University of Cambridge	CERN, Geneva
University of Glasgow	College de France
Imperial College, London	Ecole Polytechnique, France
University College, London	University of Durham
University of Liverpool	University of Edinburgh
University of Oxford	University of Glasgow
Queen Mary College, London	Imperial College, London
Rutherford High Energy Laboratory	University of Liverpool
University of Southampton	University of Oxford
University of Sussex	Rutherford High Energy Laboratory
University of Warwick	University of Strasbourg, France
Westfield College, London	Tufts University, USA
	University College, London
	Westfield College, London

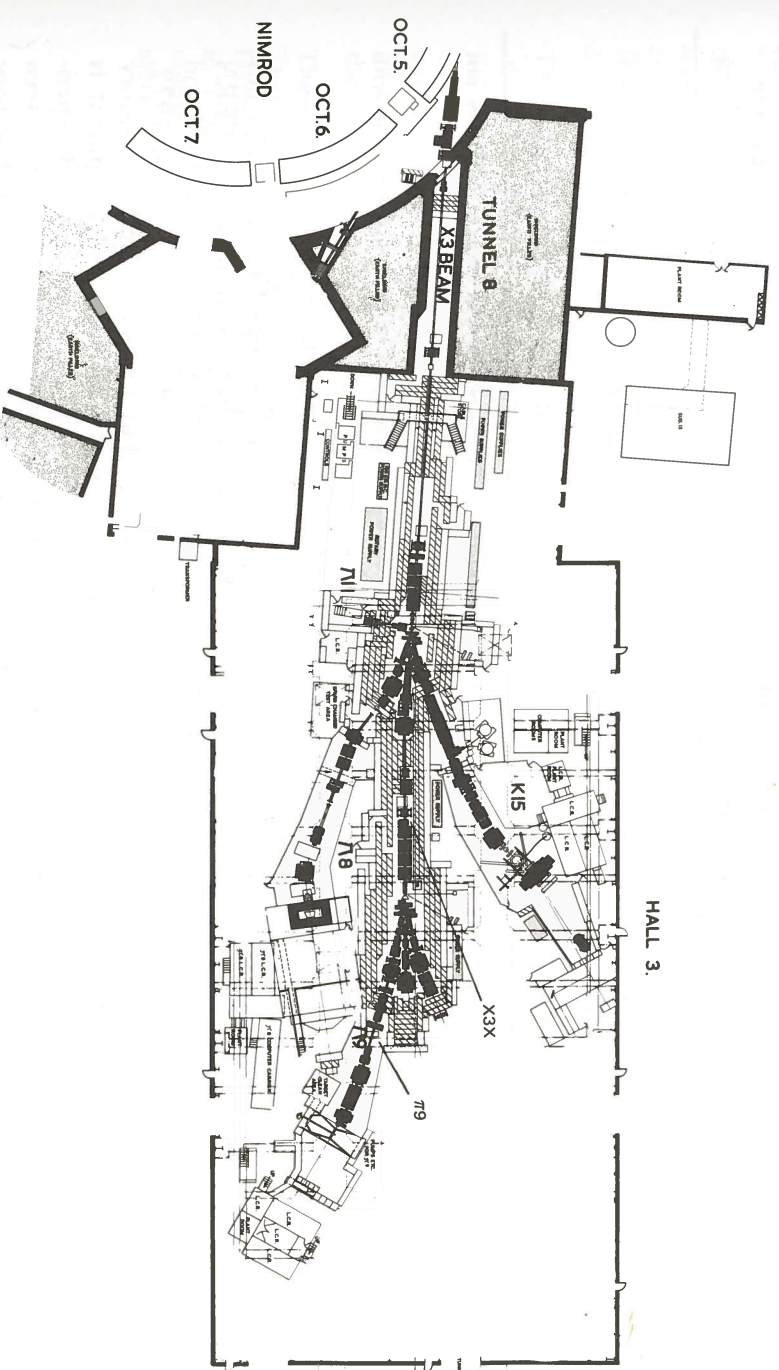


Figure 1. Beam lines in Experimental Hall 3 in January 1971. The Phase II extension of beam-lines consists of X3X (continuation of the external proton beam X3 to a second target station), beam-line $\pi 9$ together with provision for two other beam-lines, one in the forward direction. (This figure is also available in pullout form at the end of the Report).

In the other Experimental Halls (1 and 2) two important long-standing elastic scattering experiments have come to an end and have vacated their beamlines. These are:

1. The large scale πp scattering experiment using a polarized target (Experiment 4) of the RHEL/Oxford/Warwick group, which made polarization measurements at 68 momentum points, over the momentum range 0.6 GeV/c to 2.7 GeV/c. Data from this experiment is already partially analysed, and the accurate polarization measurements will prove invaluable in improving the phase shift analysis over this momentum region. The magnets used in this beamline (K14A) were needed for the Experimental Hall 3 expansion; their removal has eased congestion in Experimental Hall 1.

2. The K^- and K^+ p scattering experiment (Experiment 2) of the UCL/RHEL group which used a highly automated wire spark chamber system with core read-out, connected to an on-line computer. This experiment produced an extensive amount of elastic scattering data over 32 momentum points for K^- p scattering, and 28 momentum points for K^+ p scattering. Analysis is now well advanced, and the preliminary data has been fed into a phase shift analysis. A nuclear structure experiment (Experiment 32) has now moved into this beamline (K8 modified to $\pi 10$ in Experimental Hall 2) and data taking will commence in early 1971.

Composition of Teams using Nimrod in 1970

	Physicists		Research Students		Support Staff*	
	Electronic Techniques	Bubble Chambers	Electronic Techniques	Bubble Chambers	Electronic Techniques	Bubble Chambers
Visitors**	58	33	30	20	12	-
Resident RL staff †	30	9	-	-	22	13
TOTAL	88	42	30	20	34	13

* Includes only technical assistance directly concerned with experiments and does not include engineering support.

** Staff from Universities and other groups.

† These numbers include 31 fixed term Research Associates and 5 staff members with joint University appointments.

Experiments at CERN

A clearly developing trend is the increasing interest in using CERN shown by our counter teams. Two experiments have recently been completed at CERN (Experiments 7 and 14), two more will run in 1971 (Experiments 10 and 18) and two further experiments are being proposed and could start taking data in 1972. By the end of 1972 all nine counter teams supported by the Rutherford Laboratory are likely to have participated in experiments at CERN. This development is illustrated in Table 2 where links with CERN experiments, or proposed experiments, are listed. In one or two cases the planning is still tentative. As can be seen all the counter teams supported financially and technically by the Laboratory appear in the table, which spans a period of about four years; some groups appear more than once. It is interesting to note that many groups are amalgamating to carry out experiments at CERN and in some cases are collaborating with CERN or other European groups.

In Table 2 we can see how the various CERN commitments are developing. The first, and earliest, of the listed experiments (Experiment 14) $K^\pm \rightarrow \pi^\pm \pi^0 \gamma$ completed

Table 2

COUNTER GROUPS USING CERN

Group	Experiment	Present State	Year of Data Taking
RHEL(C)/Oxford / Liverpool/Warwick	$K^\pm \rightarrow \pi^\pm \pi^0 \gamma$ } (No. 14) $K^\pm \rightarrow \pi^\pm \pi^0 \pi^0$ }	Analysis	1969
RHEL(B)/Cambridge	π^\pm p at 300 MeV/c (No. 7)	Analysis	1970
QMC/RHEL/Liverpool/ DNPL	$\bar{p}p$ interactions (No. 10)	Mounting Apparatus	1971
UCL/RHEL(S(B)/Bristol/ Liverpool/Scandinavian Universities	ISR experiment (No. 18)	Preparing Apparatus	1971
Oxford/CERN	π and K scattering with polarized target	Data taking/ Tentative	1971
RHEL(A)/Westfield/ Birmingham	Boson studies on Omega Magnet	Design	1972
Imperial College/ Southampton/ETH	Ξ studies in Omega	Tentative	1972/3
RHEL (C)	$K^- p \rightarrow \bar{K}^0 n$ polarization	Tentative	1972/3
Birmingham/RHEL/ CERN	Kp and πp large angle scattering	Tentative	1972

data taking in autumn 1969 and the team has returned to the UK. Data analysis has been going on throughout 1970 using the Rutherford Laboratory's IBM 360/75 computer and preliminary results are given in this report. The next experiment (Experiment 7) was a detailed study of the first discovered $\pi^- p$ resonance, the $\Delta(1238)$.

This experiment completed running at the CERN synchro-cyclotron in the summer of 1970, and since that time data analysis has continued at both Cambridge and the Rutherford Laboratory. Results have already been obtained (see figures 22 and 23) and it is clear that the precision is considerably better than in all previous studies of the Δ particles. As a result it has been possible to determine the masses of the Δ 's to a substantially better accuracy than before, and to obtain a value for the electromagnetic mass splitting, for which predictions exist in SU(3) theory.

The group carrying out the $\bar{p}p$ experiment moved to CERN in the autumn of 1970. Their experimental equipment has been designed and manufactured at the Daresbury Laboratory and the Rutherford Laboratory and is shown schematically in figure 2. The large wire chambers use core read-out and are on-line to a computer. Installation will be completed by spring 1971 and data taking should start in the summer.

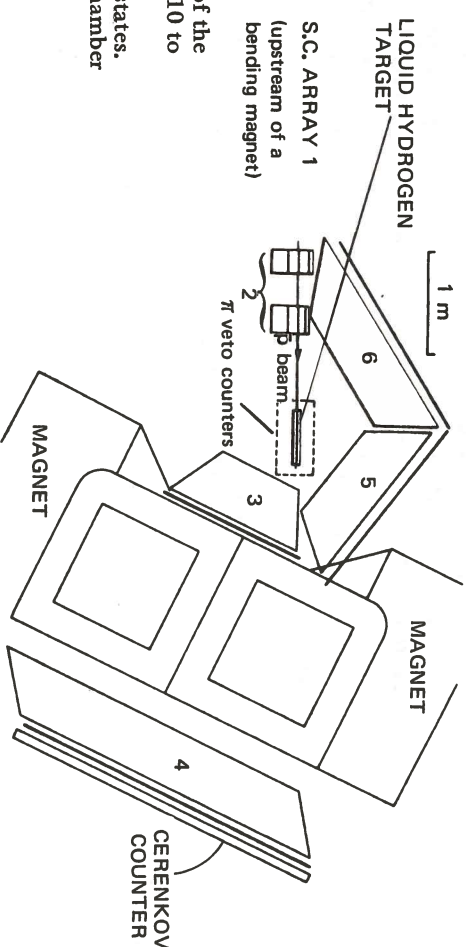


Figure 2. Schematic diagram of the apparatus used in Experiment 10 to study $\bar{p}p$ elastic scattering and annihilation into two particle states. Numbered blocks are spark chamber arrays.

Figure 3(b). Photograph taken during the construction of the large array of magnetised steel and spark chambers to be used in Experiment 18.

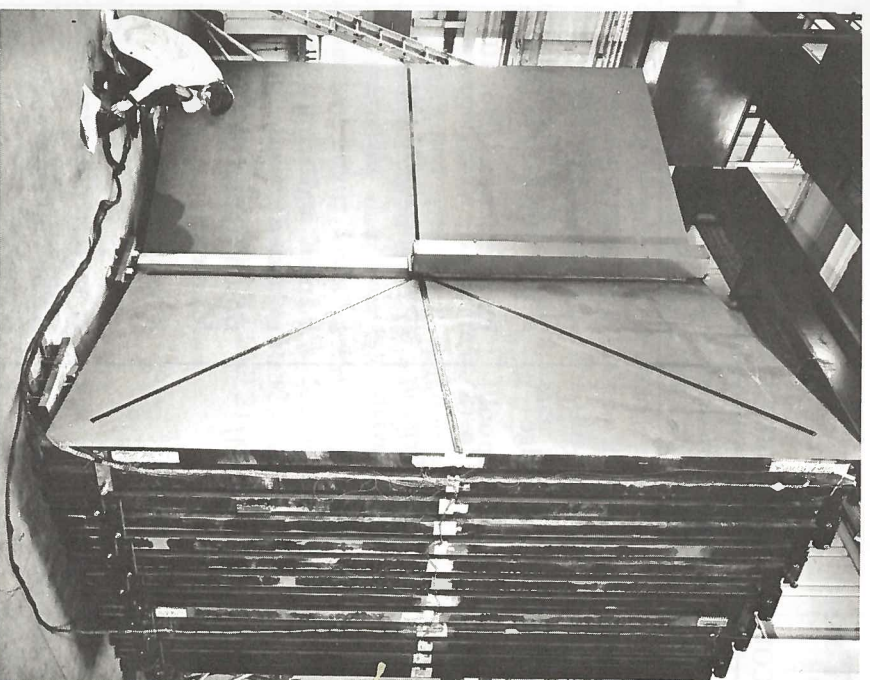
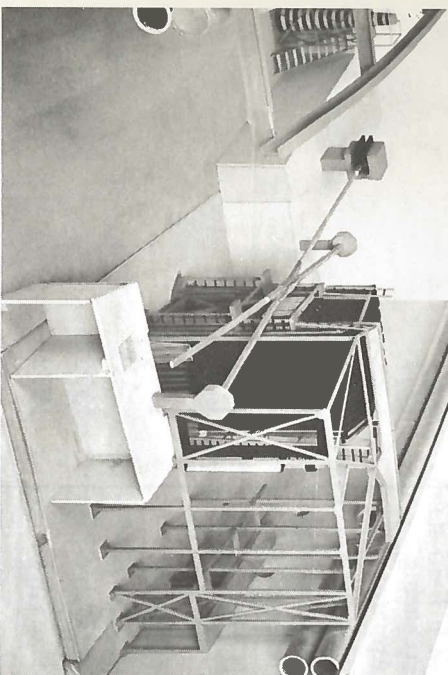


Figure 3(a). A scale model of the apparatus to be used in Experiment 18 to study production of particles at large angles to the colliding beams of the CERN Intersecting Storage Rings.



Experiments at the Intersecting Storage Rings

The construction and development programme of the Intersecting Storage Rings (ISR) at CERN is on schedule and two 15 GeV beams have already been made to interact. Experimental work is due to start in April 1971. As discussed in detail in the 1969 Annual Report, the ISR is a circular machine in which two beams of protons travelling around in opposite directions are brought into head-on collision in each of 8 intersection zones. Such a collision of two 28 GeV protons has 56 GeV of kinetic energy completely available for the production of new heavy particles. The same 'available' energy could be achieved with a conventional machine (single proton beam hitting a stationary proton target) only by going up to a beam energy of about 1500 GeV. Although the interaction probability for the colliding beams is low, the ISR will give us a glimpse of 1500 GeV physics which has hitherto been available only through cosmic ray work. The Rutherford Laboratory supported experiment at the ISR (Experiment 18) is intended primarily to search for the 'intermediate boson' (the 'messenger' particle of weak interactions) by looking for μ mesons produced around the ISR at large angles. This experiment will, in addition, study particle production at wide angles. A model of the planned apparatus is shown in figure 3a; the spark chambers are of the optical type and have dimensions up to 4 m x 2 m. The total spark chamber arrays contain 22 of the large chambers between plates of magnetized steel (figure 3b) and will weigh 300 tons.

The next experiment listed involves π and K elastic scattering studies with a polarized target. This is a CERN experiment which members of the Oxford Group have recently joined. It is hoped to continue the collaboration with further experiments.

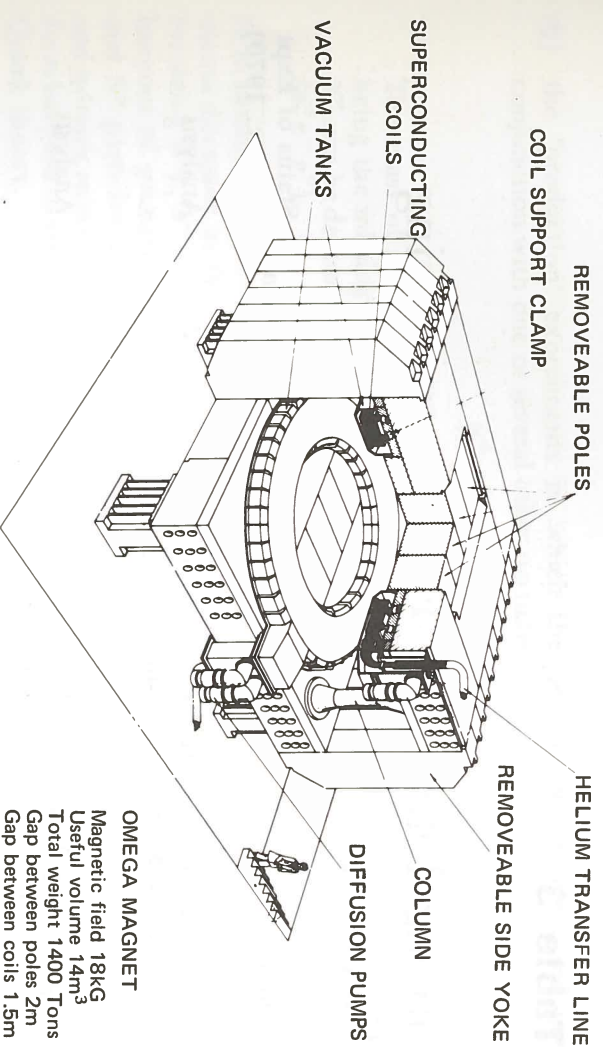


Figure 4. A scale drawing of the magnet to be used in the Omega project at CERN. (Photograph by courtesy of CERN).

Another CERN project which is coming close to fruition, and which is causing a great deal of interest, is the Omega magnet project. This is a large volume superconducting magnet producing a field of 18 kG over a volume 3 m in diameter by 2 m in height (figure 4) which will be filled by optical spark chambers. This system is built with the aim of dealing with multi-particle final states, and will have almost 4π collecting solid angle. It is believed that it will compete very strongly with the bubble chamber for multi-particle studies. The very low material density in the spark chambers (70 m radiation length) and long track length (up to 3 m) will enable very good momentum accuracy to be obtained ($\Delta p/p \pm 0.25\%$) making it superior to present day bubble chambers, and on a par with advanced design bubble chambers (e.g. the BEBC project) in momentum and mass accuracy. It will have the advantage of being a triggered device, capable of operating with high beam fluxes ($\sim 2 \times 10^5$ /burst).

For these reasons the project is gathering a large following, and some twelve experiments have been submitted for the first 2 to 3 years of running. It is interesting to note that approximately half the support comes from counter physicists and half from bubble chamber physicists.

A collaboration consisting of counter physicists from Birmingham University, Westfield College and Rutherford Laboratory with bubble chamber physicists from Birmingham University is proposing to use a 'slow neutron trigger' with Omega for the study of meson states in the mass range 1.4 to 2.2 GeV/c². Groups from Glasgow University and Liverpool University are planning to participate in an experiment with a 'slow proton trigger' which will yield complementary data.

The strong interaction experiments listed in Table 3 have as a common theme the search for new resonant states and the determination of their quantum numbers (spin, parity, isotopic spin, strangeness etc). The purpose in establishing a 'periodic table' of the particles is of course to recognise some pattern in their properties. SU(3), Quark theory, and Regge theory predict that certain patterns in mass and quantum numbers should exist, and to a large extent these patterns appear to be seen experimentally. One of the present main spheres of elementary particle physics research is to establish the properties of the large number of baryons and mesons, in order to test more carefully the truth of the theories. Should it turn out that the Quark theory is correct, and that quarks exist physically, then elementary particle physics would move one stage further, to the physics of the three quarks and their anti-quarks.

The Omega Magnet Project (ref. 173)

Strong Interaction Experiments

Table 3

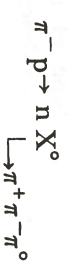
Strong Interaction Experiments using Electronic Techniques

Number	Experiment	Beam Line	Status of Expt (at Dec. 1970)
1	$K^{\pm}p$ Differential Cross-Sections in the Momentum Range 0.45 – 0.90 GeV/c	K12	Analysis
2	$K^{\pm}p$ Differential Cross-Sections in the Momentum Range 0.9 – 2.2 GeV/c (K^-) and 1.6 – 2.4 GeV/c (K^+)	K8	Analysis
3	Neutral States produced in K^-p Elastic Scattering	K10S	Analysis
4	Polarization Effects in π^+p Elastic Scattering	K14A	Analysis
5	Wide Angle Elastic pp Scattering	P71	Analysis
6	An Investigation of Narrow Width Mesons produced in πp Interactions	$\pi 7$	Analysis
7	Low Energy Pion-Nucleon Interactions	CERN	Analysis
8	K^+p Differential Cross-Sections in the Momentum Range 1 – 2 GeV/c	K15	Data Taking
9	$K^{\pm}n$ Elastic and K^+ Charge Exchange Differential Cross-Sections	K12A	Setting up
10	$\bar{p}p$ Elastic Scattering and two-body Annihilation	CERN	In preparation

These resonant searches can be classified into two experimental types:

(a) the 'formation' experiments in which bombarding and target particles (e.g. πp) coalesce to form the new particle or 'resonance' (e.g. Δ), the bombarding energy being just right for the total available energy to equal the mass of the new particle. The new particle soon decays either back to the original particles (πp , elastic scattering) or to the original particle 'types' with charges interchanged ($\pi^0 n$, charge exchange) or to different particles (e.g. $\Sigma^- K^+$, inelastic scattering).

(b) the 'production' experiments in which the new particle is produced in conjunction with one or several other particles e.g.



The mass of X^0 can be determined in this case from two body kinematics, being the missing mass to the 'other particle' (n). Alternatively the mass of X^0 can be determined from the total mass energy going to the decay particles ($\pi^+ \pi^- \pi^0$).

It is interesting to note that out of some 30 elementary particle physics experiments discussed in this year's report, no fewer than 13 are formation experiments involving $\pi^+ p$, $\pi^- p$, $K^+ p$ and $K^- p$ scattering. The $\pi^+ p$ and $\pi^- p$ scattering forms baryons of strangeness zero and isotopic spin $\frac{3}{2}$ and $\frac{1}{2}$; these are called Δ particles and N^* particles, respectively. $K^- p$ scattering can form baryons of strangeness -1 and isotopic spin 0 or 1, which are called Λ^{*} 's and Σ^{*} 's. The $K^+ p$ scattering would form baryons of strangeness $+1$ (called Z^{*} 's), which should not exist in the simplest Quark theory.

Nimrod is one of the best machines for producing high fluxes of π mesons in a momentum region which is very rich in N^* and Δ states (see Table 4). As a result physicists working at Nimrod have put a lot of effort into $\pi^+ p$ and $\pi^- p$ scattering experiments and have contributed an important part of the world data from these studies.

Table 4

Pion-Nucleon Resonances in the Nimrod Energy Range

Mass MeV/c ²	Pion Momentum MeV/c	$N^*(I=\frac{1}{2})$ JP	$\Delta(I=\frac{3}{2})$ JP
1236	304		$\frac{3}{2}^+$
1470	660	$\frac{1}{2}^+$	
1520	740	$\frac{3}{2}^-$	
1535	760	$\frac{1}{2}^-$	
1650	960	$\frac{1}{2}^-$	$\frac{1}{2}^-$
1670	1000		$\frac{3}{2}^-$
1670	1000		
1688	1030	$\frac{3}{2}^+$	
1700	1050	$\frac{1}{2}^+$	
1780	1200	$\frac{1}{2}^+$	
1860	1360	$\frac{3}{2}^+$	
1890	1420		$\frac{5}{2}^+$
1910	1460		$\frac{1}{2}^+$
1950	1540		$\frac{3}{2}^+$
1990	1630		
2040	1730	$\frac{1}{2}^+$	
2190	2070	$\frac{3}{2}^-$	
2420	2640		$\frac{1}{2}^+$
2650	3260		
2850	3850		

It is of interest to look at the impact of Rutherford Laboratory work in this field. A list of all the π^-p experiments performed up to the present time at Rutherford Laboratory is given in Table 5a. The type of interaction process is listed in the fifth column; in the majority are those described as $\pi^{\pm}p \rightarrow \pi^{\pm}p$, i.e. simple elastic scattering experiments; there are two cases of experiments which are described as 'inelastic' or 'quasi-elastic' processes, and there are two cases of charge exchange scattering ($\pi^-p \rightarrow \pi^0n$).

In the field of 'formation' studies the first experiments are always simple total cross-section measurements. In these the loss of beam particles in passing through a hydrogen target is measured as a function of beam energy. The principle is that whenever the beam energy goes through a value where the particles (πp) coalesce into some new N^* or Δ a 'resonance' will occur and the cross-section will show a peak. Such behaviour is seen in the graphs of π^+p and π^-p total cross-sections shown in figure 5. Peaks which imply resonances are visible at energies of 1920 MeV in the π^+p case and 1512 MeV and 1688 MeV in the π^-p case. At the time when Nimrod became operational (August, 1963) these, with the $\Delta(1238)$, were the only known Δ or N^* baryons, and many of the early experiments at Nimrod were designed to investigate their properties.

Table 5a

Experiments on πN scattering carried out in the 7 years of operation of Nimrod

Beam	Measurement*	Reaction	Momentum (GeV/c)	Team
$\pi 1$	$\frac{\partial \sigma}{\partial \Omega}$	$\pi^{\pm}p \rightarrow \pi^{\pm}p$	0.88 to 1.58	RHEL
$\pi 2$	P_0 $\frac{\partial \sigma}{\partial \Omega}$	$\pi^-p \rightarrow \pi^-p$ $\pi^{\pm}p \rightarrow \pi^{\pm}p$	1.72 to 2.8	UCL/Westfield
$\pi 3$	$\frac{\partial \sigma}{\partial \Omega}$	$\pi^-p \rightarrow \pi^0n$	1.7 to 2.5	Oxford
$\pi 5$	$\frac{\partial \sigma}{\partial \Omega}$	$\pi^-p \rightarrow \pi^-p$	1.5 to 3.5	Bristol/RHEL
$\pi 6$	σ_{TOT}	$\pi^{\pm}N$	0.5 to 2.65	Cambridge/Bham/RHEL
$\pi 7$	P_0	$\pi^-p \rightarrow \pi^-p$	0.64 to 2.09	RHEL
$\pi 7'$	P_0	$\pi^-p \rightarrow \Sigma^-K^+$	1.13	AERE/QMC/RHEL
$\pi 14$	P_0	$\pi^+p \rightarrow \Sigma^+K^+$	1.11	Westfield/RHEL
$\pi 5$	$\frac{\partial \sigma}{\partial \Omega}$	$\pi^-p \rightarrow \pi^-p$	1.5 to 3.5	Bristol/RHEL
$\pi 1 + HBC$	inelastic processes	$\pi^{\pm}p$	0.6 to 1.2	Imperial/Westfield/Oxford/Saclay
$\pi 14A$	P_0	$\pi^+p \rightarrow \pi^+p$	0.62 to 2.69	RHEL/Oxford
$\pi 9 + HBC$	inelastic processes	π^+p	1.1 to 1.9	Westfield/Imperial College
$\pi 15$	$\frac{\partial \sigma}{\partial \Omega}$	$\pi^+p \rightarrow \pi^+p$	0.6 to 2.0	Bristol/RHEL
$\pi 9$	P_0	$\pi^-p \rightarrow \pi^0n$	0.6 to 3.0	RHEL/Glasgow
$\pi 8$	$\frac{\partial \sigma}{\partial \Omega}$	$\pi^{\pm}p \rightarrow \pi^{\pm}p$	1.0 to 1.4	UCL/RHEL

* $\frac{\partial \sigma}{\partial \Omega}$: measurement of angular distributions

P_0 : measurement of polarization effects using a polarized target

σ_{TOT} : measurement of total cross-section

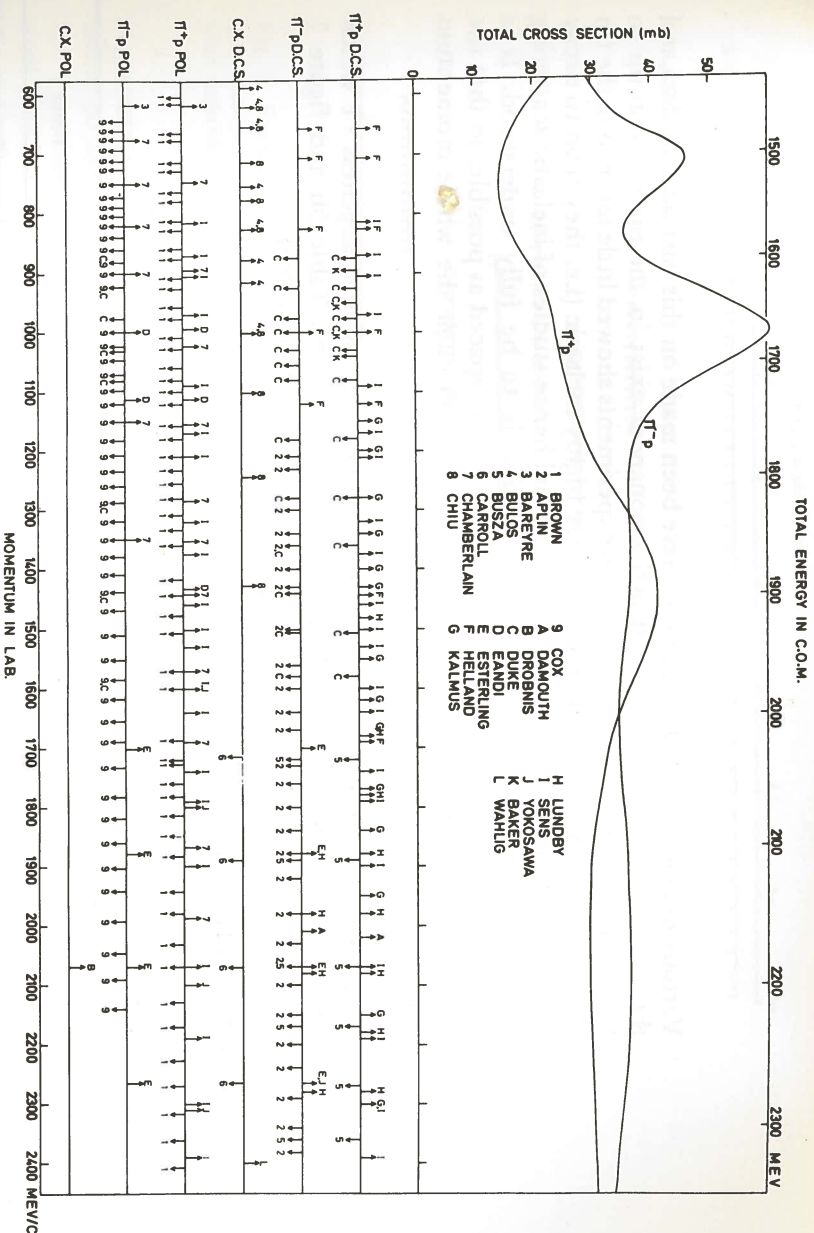


Figure 5. Summary of the world data on πp elastic scattering measurements in the range 600 to 2400 MeV/c. The arrows below the line indicate measurements made at RHEL; arrows above the line indicate measurements at all other laboratories.

In these experiments angular distributions and polarization effects were measured, which then allowed the very powerful phase shift analysis method to be applied to the unravelling of particle states of different spin. It very quickly became clear from the results of these early experiments that the broad peaks in the total cross-section graphs contained several resonances superimposed on each other. In particular the 1688 MeV peak in the π^-p cross-section was found to be dominated by two resonances, and in fact a total of four resonances were finally shown to exist in this small region. With this work came the realisation that in the πN system there existed a very large number of resonance states (this also implies via SU(3) theory that an equally large number of strange baryons Σ^* , Λ^* , Σ^* should exist). As is shown in the table this work has progressed vigorously at RHEL with polarization and differential scattering experiments of increasing accuracy and increasing numbers of momentum settings being performed. A typical angular distribution curve is shown in figure 6; some typical polarization measurements are shown in figure 15. Referring back to figure 5, the arrows below the line show momentum points at which measurements have been made at RHEL, and those above the line represent measurements at all other laboratories; RHEL is seen to have produced approximately one half of the world's data.

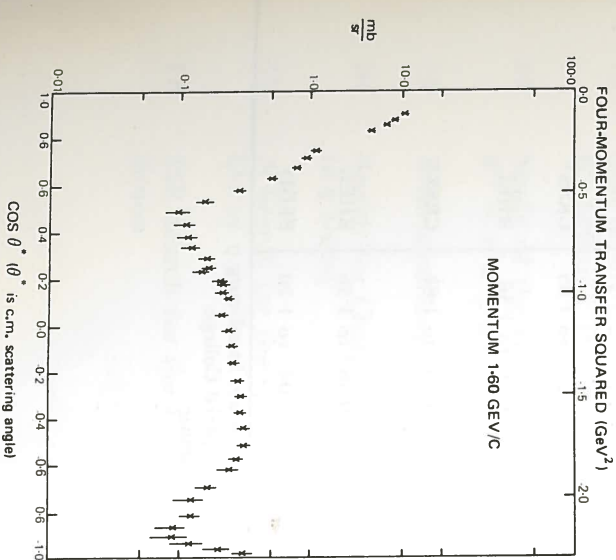


Figure 6. π^-p Differential cross-section measurements made at 1.60 GeV/c from Aplin et al (Experiment No. 1, 1969 Annual Report).

Various detailed phase shift analyses have been made on this vast bulk of data and the results show that at least 20 π N resonances exist in the mass region up to 2.85 GeV/c². The first total cross-section experiments showed little more than the tip of the iceberg. Many of the resonances are highly inelastic (i.e. they tend to decay to other channels rather than back to π p) and hence studies of inelastic scattering are essential if this rather complex situation is to be fully understood. It is invaluable to have the momentum points as closely spaced as possible, so that the phase shift analysis can be continued smoothly through the whole momentum scale.

A similar situation exists with respect to the baryons with strangeness -1 which have to be studied through K^-p and K^-n interactions. Table 5b and figure 7 summarises the Rutherford Laboratory contribution to this field.

Table 5b

Experiments on KN interactions in the momentum range up to 2.5 GeV/c

Reference on figure 7	Experiment No. in this report	Measurement ϕ	Reaction	Momentum (GeV/c)	Team
A	(Beam K6)	σ_{TOT}	K^-p and K^-n	0.59 to 2.66	Bham/Cambridge/RHEL
B	1	$\frac{d\sigma}{d\Omega}$	$K^-p \rightarrow K^-p$	0.62 to 0.94	Birmingham/RHEL
C	2	$\frac{d\sigma}{d\Omega}$	$K^-p \rightarrow K^-p$	1.12 to 1.40 and 1.75 to 2.45	University College/RHEL
D	19	$\frac{d\sigma}{d\Omega}$	$K^-p \rightarrow K^-p$	1.25 to 1.85	CRSS*
E	20†	$\frac{d\sigma}{d\Omega}$	$K^-p \rightarrow K^-p$	0.96 to 1.36	RHEL
F	25	$\frac{d\sigma}{d\Omega}$	$K^-n \rightarrow K^-n$	1.04 to 1.70	Glasgow/Imperial College
G	(Beam K7)	$\frac{P}{d\Omega}$	$K^-p \rightarrow K^-p$	1.085 to 1.370	Oxford/RHEL
D	19	$\frac{d\sigma}{d\Omega}$	$K^-p \rightarrow \Lambda\pi^0$	1.25 to 1.85	CRSS*
F	25	$\frac{d\sigma}{d\Omega}$	$K^-n \rightarrow \Lambda\pi^-$	1.04 to 1.70	BEG†
H	3	$\frac{d\sigma}{d\Omega}$	$K^-p \rightarrow \Lambda\pi^0$	0.685 to 0.990	Oxford
E	20†	$\frac{d\sigma}{d\Omega}$	$K^-p \rightarrow \Lambda\pi^0$	0.96 to 1.36	RHEL
H	3	$\frac{d\sigma}{d\Omega}$	$K^-p \rightarrow \Sigma^0\pi^0$	0.685 to 0.990	Oxford
D	19	$\frac{d\sigma}{d\Omega}$	$K^-p \rightarrow \Sigma^+\pi^-$	1.25 to 1.85	CRSS*
E	20‡	$\frac{d\sigma}{d\Omega}$	$K^-p \rightarrow \Sigma^+\pi^0$	0.96 to 1.36	RHEL
D	19	$\frac{d\sigma}{d\Omega}$	$K^-p \rightarrow \Lambda\omega$ $\rightarrow Y^*\pi$ $\rightarrow K^*N$	1.25 to 1.85	CRSS*
E	20†	$\frac{d\sigma}{d\Omega}$	$K^-p \rightarrow \Lambda\omega$ $\rightarrow Y^*\pi$ $\rightarrow K^*N$	0.96 to 1.36	RHEL
F	25	$\frac{d\sigma}{d\Omega}$	$K^-n \rightarrow Y^*\pi$	1.04 to 1.70	BEG†

*CRSS : Collaboration of College de France, Rutherford Lab., Saclay, Strasbourg.

†BEG† : Collaboration of Birmingham, Edinburgh, Glasgow, Imperial College.

‡Film for this experiment obtained from CERN 2 m bubble chamber.

ϕ σ_{TOT} : measurement of total cross-section.

$\frac{d\sigma}{d\Omega}$: measurement of differential cross-section.

$\frac{P}{d\Omega}$: measurement of polarization $\times \frac{d\sigma}{d\Omega}$

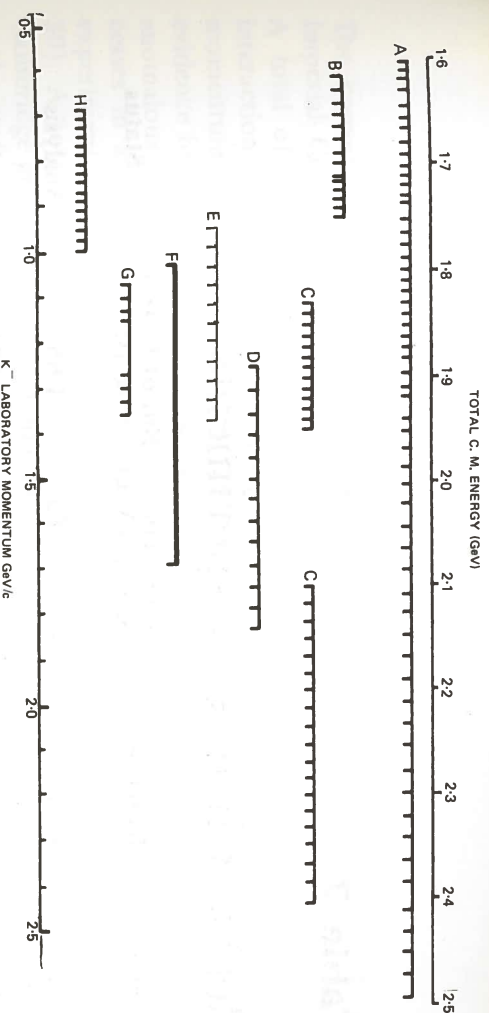


Fig. 7. Summary of Rutherford Laboratory measurements on the KN interaction. The vertical marks indicate the momentum points at which measurements have been made. The experiments with unbroken horizontal bars had a continuous effective momentum coverage.

Approximately one quarter of the experiments discussed in this year's report relate to the weak and electromagnetic interactions. A central feature for most of the experiments has been the search for small violations to the normal, and quite well understood, weak and electromagnetic interactions. Most of these experiments are in an analysis or data taking stage, and should produce intermediate or final results during 1971.

Weak Interaction Experiments

Table 6

Weak and Electromagnetic Interaction Experiments using Electronic Techniques

Number	Experiment	Beam Line	Status of Expt. (at Dec. 1970)
11	A Measurement of the Electron Asymmetry Parameter of the Polarized Σ^-	π^4	Analysis
12	Test of the $\Delta I = \frac{1}{2}$ Rule in the Decay $\Sigma^+ \rightarrow p\pi^0$	K14	Analysis
13	Test of the $\Delta S = \Delta Q$ Rule for K^0 Leptonic Decays	K13	Analysis
14	Study of the Decay Modes $K^\pm \rightarrow \pi^\pm \pi^0 \gamma$ and $K^\pm \rightarrow \pi^\pm \pi^0 \pi^0$	CERN	Analysis
15	Bremsstrahlung Anomalies	K13B	Analysis
16	Search for Charge Asymmetry in η Decay	π^8	Data Taking
17	A Search for the C-violating Decay $\eta \rightarrow \pi^0 e^+ e^-$	π^8	Setting up
18	ISR Search for the Intermediate Boson	CERN	In Preparation

Table 7

Bubble Chamber Experiments

Number	Reaction	Momentum Range (GeV/c)	No. of Pictures $\times 10^6$	Status
19	K^-p	1.25 to 1.85	1.65	Analysis
20	K^-p	0.96 to 1.36	0.43	Analysis
			at CERN	
21	$\bar{p}p$	1.23 to 1.43	0.1	Analysis
			at CERN	
22	K^-p	14.25	0.35	Analysis and data taking
			at CERN	
23	π^+d	4.0	0.42	Analysis and data taking
			at CERN	
24	π^+p	0.8 to 1.7	0.62	Analysis
25	K^-d	1.45 and 1.65	0.71	Analysis
26	K^+p K^+d	2.1 to 2.9 2.2, 2.45, 2.7	0.21 0.92	Analysis Analysis
27	np	1.0 to 7.5	0.11	Analysis
28	np	1.0 to 3.5	0.09	Analysis
29	K^- in heavy liquid	2.2	0.68	Analysis
30	Anomalies in electromagnetic processes		0.31	Analysis
31	Development of Neon-hydrogen track sensitive target facility for 1.5 m hydrogen chamber.			

1.5 m Bubble Chamber Programme

The programme for the 1.5 m hydrogen bubble chamber has been concerned largely with the development of the track sensitive target facility, whilst the CERN 2 m chamber provided the bulk of conventional film for analysis. Nevertheless the 1.5 m chamber has produced over a million conventional pictures for four experiments during 1970, about half being taken with the chamber filled with hydrogen and half with the chamber filled with deuterium. This is to be compared with the British groups use of CERN which yielded 1.86 million pictures. The chamber has therefore contributed more than one third of the film for analysis in the UK during the year in addition to its major development programme.

Bubble Chamber Experiments

The conventional high energy physics programme saw the completion of the Imperial College/Westfield College K^+p and K^+d experiment (Experiment 26). A total of 920,000 pictures of K^+d interactions and 210,000 pictures of K^+p interactions have been taken to study the K^+N interaction in the centre of momentum energy range 2270 to 2540 MeV. The preliminary results show no evidence for the formation of exotic resonances. The Cambridge group observed anomalous behaviour of the electron bremsstrahlung and pair production processes in a test exposure made in 1969 and this has been followed up by an experiment in hydrogen using positrons and electrons at 1 GeV/c (Experiment 30). A total of 310,000 pictures were taken and analysis is in progress. The Cambridge group also received 90,000 pictures taken with a neutron beam for the analysis of inelastic np channels (Experiment 28). Finally an exposure of 133,000 pictures went to the Imperial College/Westfield collaboration for a further study of the π^+p interaction in the range 0.8 to 1.25 GeV/c (Experiment 24).

Two attempts were made during 1970 to operate the track sensitive target facility. It had been hoped that this system would be productive for high energy physics during 1970; however difficulties with chamber filling and operation occurred which have necessitated some development work. Experiments were performed to test filling procedures, and a procedure developed to give $\approx 1\%$ variation in the stopping power of the mixture with height in the chamber. An understanding of the reasons for target failure in the June/July runs has led to a major overhaul of the chamber top-plate seals and a slight modification of the target design to include a cooling loop. This allows direct control of the temperature of the liquid inside the target.

During the past year partial wave analyses have been completed on the two body final states of the K^-p survey experiment (Experiment 19). New results include a measured width of 300 MeV for the $\Lambda^*(2100)$ and a large elasticity of 0.15 for the $\Sigma^*(1915)$ from analysis of the elastic channel. Other possible resonances require confirmation from further experiments. This experiment has been extended to lower energies with new film taken in the CERN 2 m hydrogen bubble chamber (Experiment 20).

The 14 GeV/c K^-p experiment has produced a measurement of the K^-p elastic total and differential cross-section (Experiment 22) with greatly improved accuracy over previous counter experiments in this region. This experiment will acquire more pictures in 1971. The new 4 GeV/c π^+d experiment (Experiment 23) received the first half of its requested pictures (0.8×10^6) from the CERN 2 m chamber.

The Bubble Chamber Film Analysis Facilities

The film analysis facilities at RHEL have been considerably improved in the past year. The film is scanned for interactions which are classified according to topology and then measured either manually or automatically with high precision. The large quantity of film involved and the need for high statistics makes automatic measurement, giving both speed and precision, imperative. The principle source of data is the HPD flying spot digitiser preceded by scanning and a fast manual rough digitiser stage.

The main effort during 1970 has been concentrated on improving the throughput of the combined rough digitiser — HPD system. This year has seen the installation of 6 new rough digitisers to provide guidance measurements for the HPD bringing the total to 12 digitisers at present in operation. All 12 are connected to the IBM 1130 computer which collects and checks the measurements from all machines. The 1130 programs allow for on-line scanning and calibration of the digitisers. The average event measuring rate has increased by over 50% since the system went on-line. A necessary accompaniment to this increased sophistication has been regular scheduled maintenance of the equipment.

A semi-automatic method of handling scanning information has been introduced which is designed to handle of the order of 20,000 events per week with the minimum of operator intervention. A parallel program has been developed to provide scanning efficiencies as a function of scanner, event topology, scan-table, etc, in a quickly accessible form. This allows a constant check to be maintained on the performance of the whole scanning system.

The HPD programming chain has seen continued improvements to increase the overall efficiency; in particular, a reduction in computer CPU time of the order of 20% has been achieved for the CERN filter program HAZE. Ionisation measurements from the HPD system are in routine use as an aid to the kinematic fitting. A light pen 'patch-up' system is used in production to increase the HAZE pass rate for events from approximately 70% to 85% for a single pass.

The throughput of the film analysis laboratory as determined from the number of events passing successfully through the HAZE program is given for the year in figure 8. The total number of events measured in the calendar year 1970 exceeds 200,000.

Two film plane manual digitisers have also been installed during the year and have proved of great value for the measurement of events which present the HPD with some difficulty. The machines have also been in demand for spark chamber film analysis.

The events measured in 1970 have been distributed between three experiments ranging from the 0.96 to 1.36 GeV/c K^- survey up to the 14.3 GeV/c $K^- p$ experiment; the latter being the highest energy K^- experiment so far attempted by any group. These experiments are described in the subsequent sections of this report.

Figure 8. Monthly output of the Rutherford Laboratory Bubble Chamber Film Analysis System in 1970.

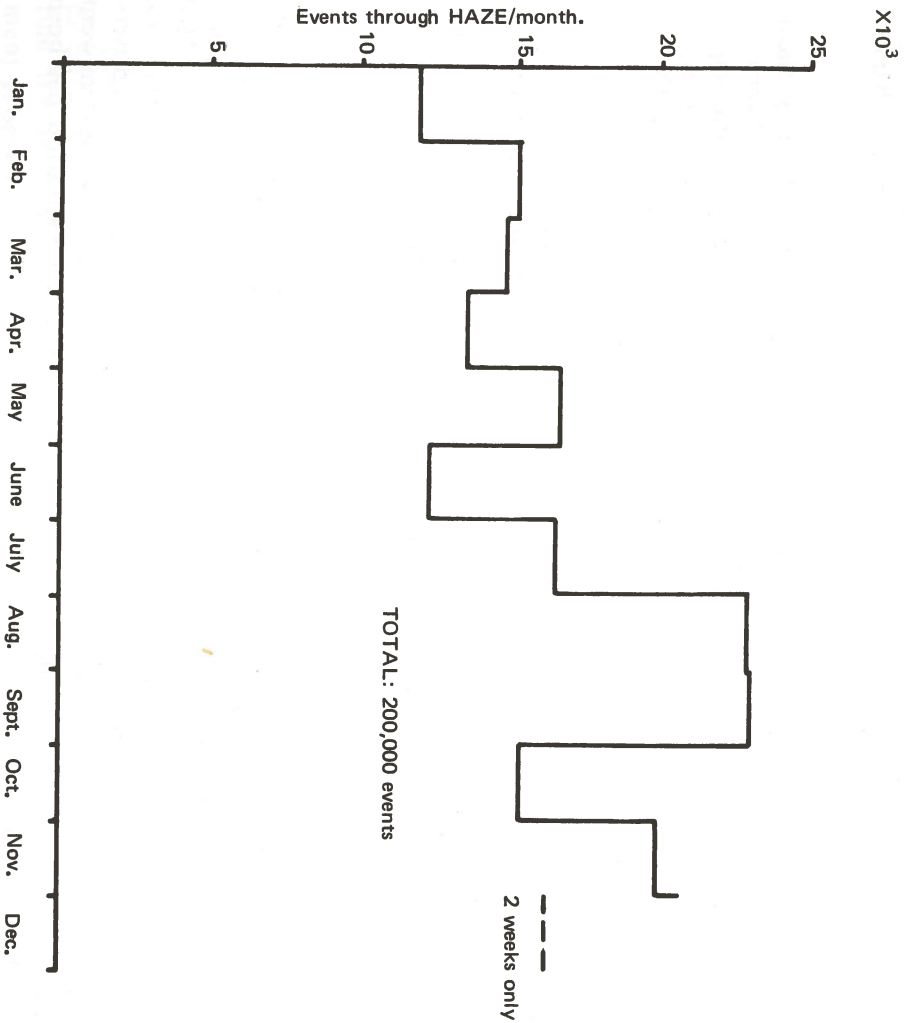


Table 8
Nuclear Structure Experiments

Number	Experiment	Accelerator	Status
32	Total Reaction Cross-Sections for Pions on Nuclei	π 10 beam Nimrod	Setting up
33	A Search for Superheavy Elements	CERN Proton Synchrotron	Data taking
34	Neutron-Proton Bremsstrahlung	AERE 110 inch Synchro-Cyclotron	Data taking/ Analysis
35	Medium Energy Nucleon Reaction Studies	Tandem Van de Graaf and AERE Variable Energy Cyclotron	Data taking/ Analysis

With the closure of the 50 MeV Proton Linear Accelerator (PLA), mentioned in the 1969 Annual Report, the Rutherford Laboratory ceased to have a machine specifically designed for studies in nuclear structure physics. However, the Laboratory continues to take an active interest in this field through the resident Nuclear Physics Group. The activities of this group now mainly lie in the use of high energy particle beams, from accelerators such as Nimrod, for studies of the structure and properties of atomic nuclei. Two such experiments are described below. One of these uses high energy pion beams from Nimrod in a measurement of total reaction cross-sections to gain further information about the density distribution of neutrons in nuclei. The other experiment uses targets irradiated in 24 GeV proton beams from the CERN Proton Synchrotron in an attempt to produce, by secondary reactions in the targets themselves, the very heavy nuclei which it has recently been suggested should exist in the region around $Z = 114$.

The Laboratory also actively supports some of the university groups using the accelerators available at AERE, in particular, those groups which previously used the PLA for nuclear physics research. Two members of the resident group have collaborated with a combined AERE/Queen Mary College, London, group to use high energy neutron beams from the 140 MeV Synchro-Cyclotron for studies of elastic and inelastic neutron — proton scattering. Active support has also been given to a combined team based on the Kings College, London, group who have carried out a variety of experiments concerned with nuclear reactions and scattering at medium energies on the Tandem Van de Graaf and Variable Energy Cyclotron at AERE. Groups from the universities of Birmingham and Manchester have also used the Laboratory's computing facilities to complete the analysis of experiments originally carried out using the PLA.

Publications associated with the various experiments, described in the following pages, are indicated by marginal reference numbers linked to the List of Publications at the end of the Report.

Experiment 1

UNIVERSITY OF BIRMINGHAM
RUTHERFORD LABORATORY

K⁺p Differential Cross Sections in the Momentum Range 0.45 to 0.90 GeV/c (ref. 4, 103, 104, 126, 136)

The purpose of these experiments on K^-p and K^+p elastic scattering is to improve the accuracy of the data in a region where many Y^* resonances have been found, or are suspected, and to clarify the question of possible structure in the K^+p cross-section which might have a bearing on the existence of the controversial Z^* resonances.

Data taking has been completed for these two experiments. The detection system used included sonic spark chambers to measure the differential scattering cross-sections for K^+p scattering at 13 momenta between 430 and 930 MeV/c, and for K^-p scattering at 14 momenta between 600 and 930 MeV/c. Analysis of these data has proceeded during 1970 in parallel with the setting up of a related experiment (Experiment 9) to measure K^+n scattering over the same momentum range.

Two arrangements were used, and angular distributions from one of these, the correlation mode, at centre of momentum angles in the range $-0.7 \leq \cos \theta^* \leq 0.7$, have been extracted from the data. These results improve on the statistics of previous data in the same momentum region by factors of between 4 and 20. There remain some corrections, affecting primarily the absolute values of the results which are still being studied. Typical distributions are shown in figure 9.

The analysis of the data for forward and backward angles has involved a careful study of systematic effects in the spark chambers which affect the accuracy of momentum fitting. Good momentum resolution is essential to separate elastic events as well as possible from the high background of kaon decays. Figure 10 shows a typical momentum distribution and illustrates the way in which this separation is achieved.

The data at low momenta are of sufficient statistical quality to determine unambiguously the sign of the K^+p Coulomb interference which was poorly measured in previous experiments. Preliminary results at one momentum (476 MeV/c) indicate a positive sign. This information will help to reduce the number of possible phase shift solutions.

Figure 10. Momentum distribution of tracked particles through the spectrometer magnet of Experiment 1. The momentum of the incident K beam was -800 MeV/c and the selected particles have angles of about 7° to the incident beam in the laboratory reference frame.

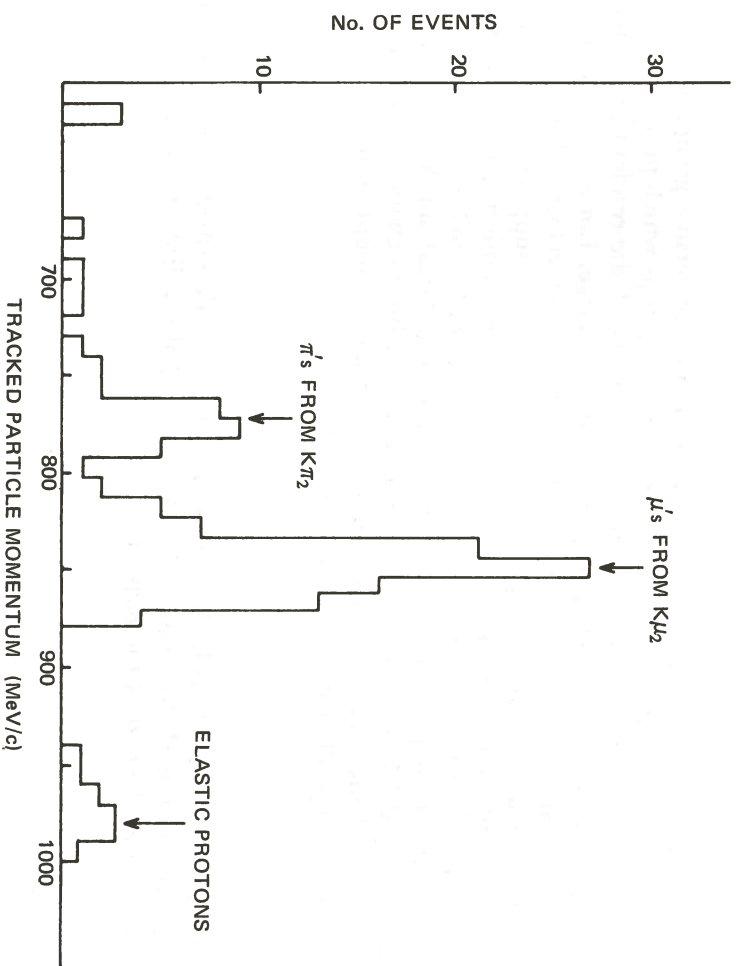
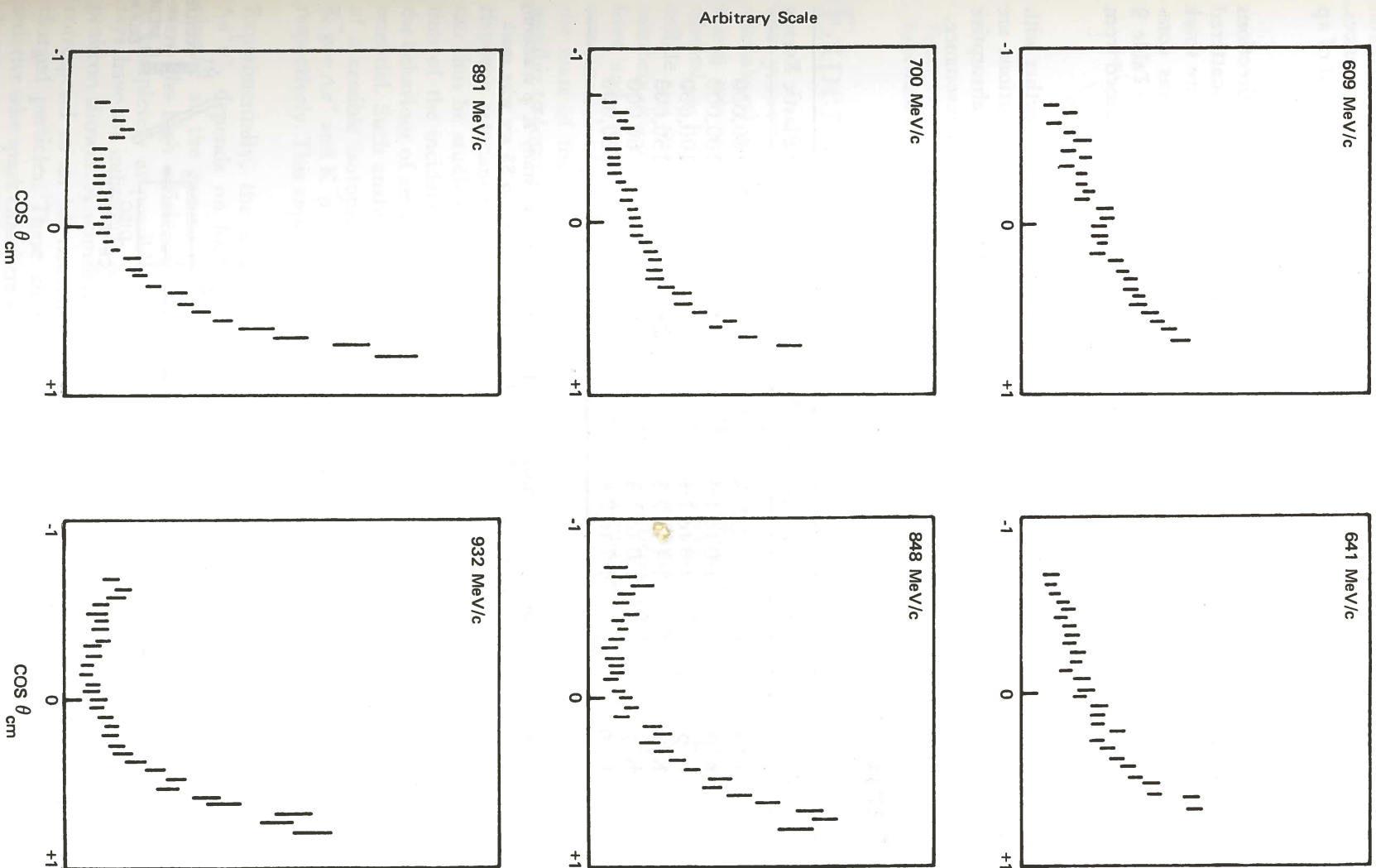


Figure 9. Typical angular distributions for K^-p elastic scattering from Experiment 1, with correlation geometry. The statistical quality considerably exceeds earlier experiments. Absolute normalisation is being finalised.



Experiment 2

UNIVERSITY COLLEGE, LONDON
RUTHERFORD LABORATORY

K⁺p Differential
Cross-Sections in the
Momentum Range
0.9 to 2.2 GeV/c (*K⁻*) and
1.6 to 2.4 GeV/c (*K⁺*)

The aim of this particular group of experiments is the measurement of the differential cross-sections of *K⁺p* and *K⁻p* elastic scattering over a wide range of momenta to provide data to assist in the classification of some of the hyperon resonances and search for effects due to possible 'exotic' *Z^{*}* resonances. The range of measurements made is shown in table 9. A substantial amount of π data was obtained as a useful by-product.

The experimental arrangement is shown in figure 11. Incident particle directions were determined by two counter hodoscopes (H1 and H2) and particles scattered from a 15 cm liquid hydrogen target were detected by core read-out wire spark chambers (S1 to S8) on-line to a PDP-8 computer. Data acquisition was completed in May 1970 and the analysis has reached an advanced stage. Table 9 summarises the experiments and gives the number of elastic events obtained from the raw data.

A phase shift analysis was performed on the *K⁺p* preliminary data together with existing data and four solutions were found (figure 12). The solutions are characterised by partial wave amplitudes which become increasingly absorptive with increasing momentum and no solution gives any evidence of a *Z₁^{*}* resonance.

Table 9

Process	Momentum GeV/c	No. of Momenta	No. of Elastic Events
π^+p	1.715	1	60,000
π^+p	1.0 to 1.4	14	100,000
π^-p	1.0 to 1.4	14	100,000
K^+p	1.4 to 2.3	28	150,000
K^-p	1.0 to 1.4	13	60,000
K^-p	1.7 to 2.4	19	80,000

Figure 11. Schematic diagram of the apparatus used in Experiment 2 to study *K⁺p* scattering. C1 to C5 are scintillation counters, V1 to V5 are veto counters and S1 to S8 are wire spark chambers.

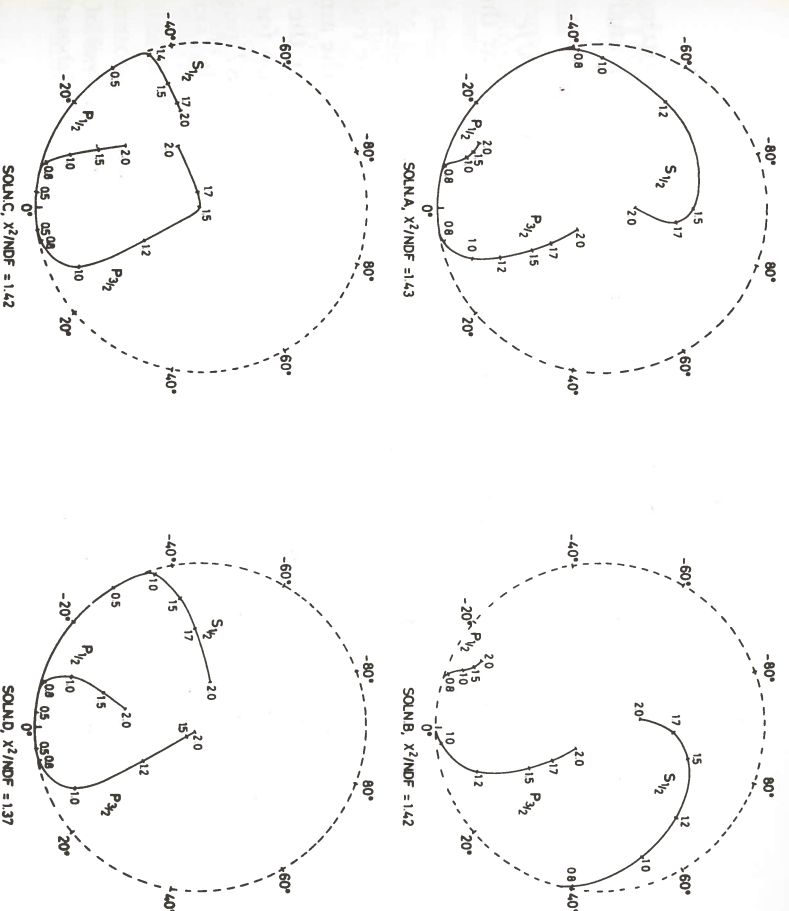
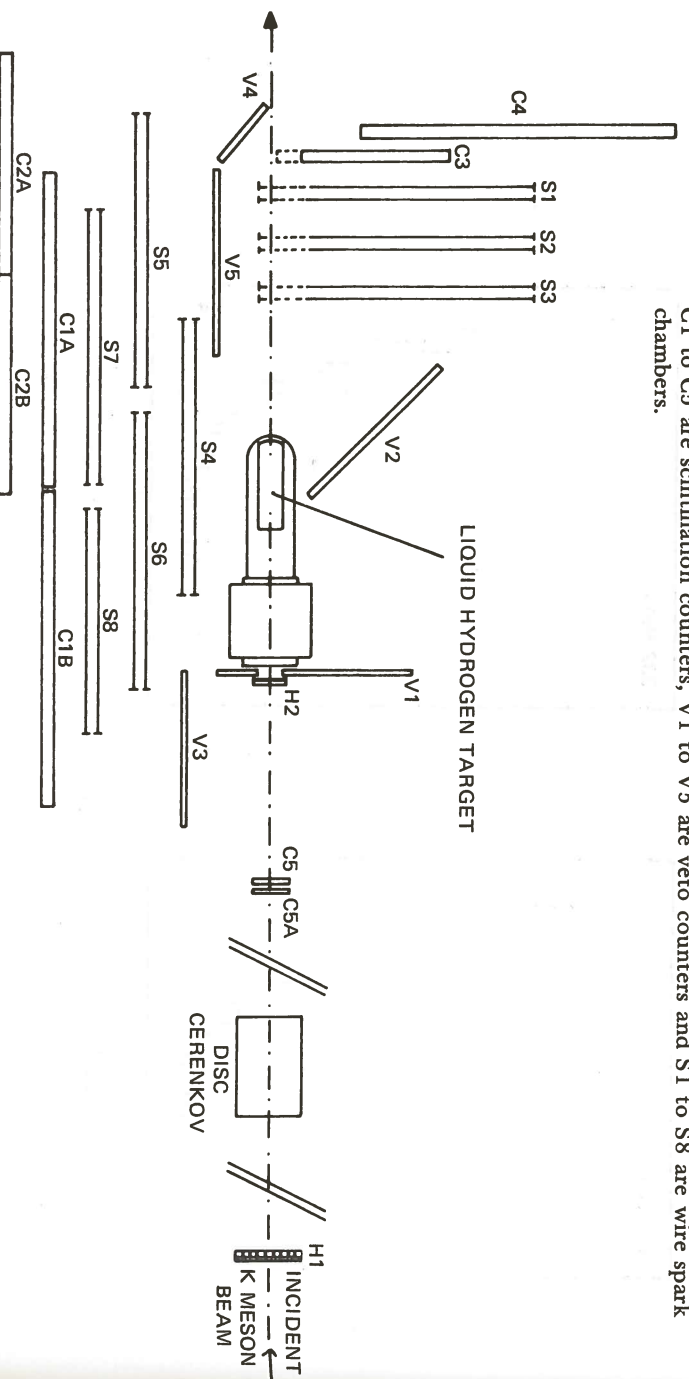


Figure 12. Four solutions found from phase shift analysis of the *K⁺p* preliminary data from Experiment 2 together with existing data.

Experiment 3

UNIVERSITY OF OXFORD

*Neutral States
Produced in K⁻p
Elastic Scattering*

The properties and quantum numbers of unstable particles (loosely called resonances) are of considerable interest in the study of the systematics of the strong interactions. If it is experimentally possible, these resonances are best studied in 'formation' experiments wherein a target particle and a missile particle collide and coalesce to form a new particle or resonance, which then has quantum numbers that are the sum of those of the initial particles. The new particle is short lived and soon decays either back to the two original particles or to some other combination of particles. The total energy available in the collision corresponds to the mass of the particle formed. By working at a series of beam energies it is possible to form a range of new particles.

Hyperon resonances can decay into $\bar{K}N$, as well as other channels such as $\Lambda\pi$ and can thus be studied by careful analysis of K^-p formation experiments, as a function of the incident K^- momentum. A partial wave analysis, which projects out the behaviour of amplitudes with specific angular momentum quantum numbers is essential. Such analysis is simplified by looking at processes in which the number of accessible isotopic spin quantum states is restricted. Two such channels are $K^-p \rightarrow \Lambda\pi^0$ and $K^-p \rightarrow \Sigma^0\pi^0$ where the isotopic spin is restricted to $I = 1$ and $I = 0$ respectively. This experiment concentrates on these two interactions.

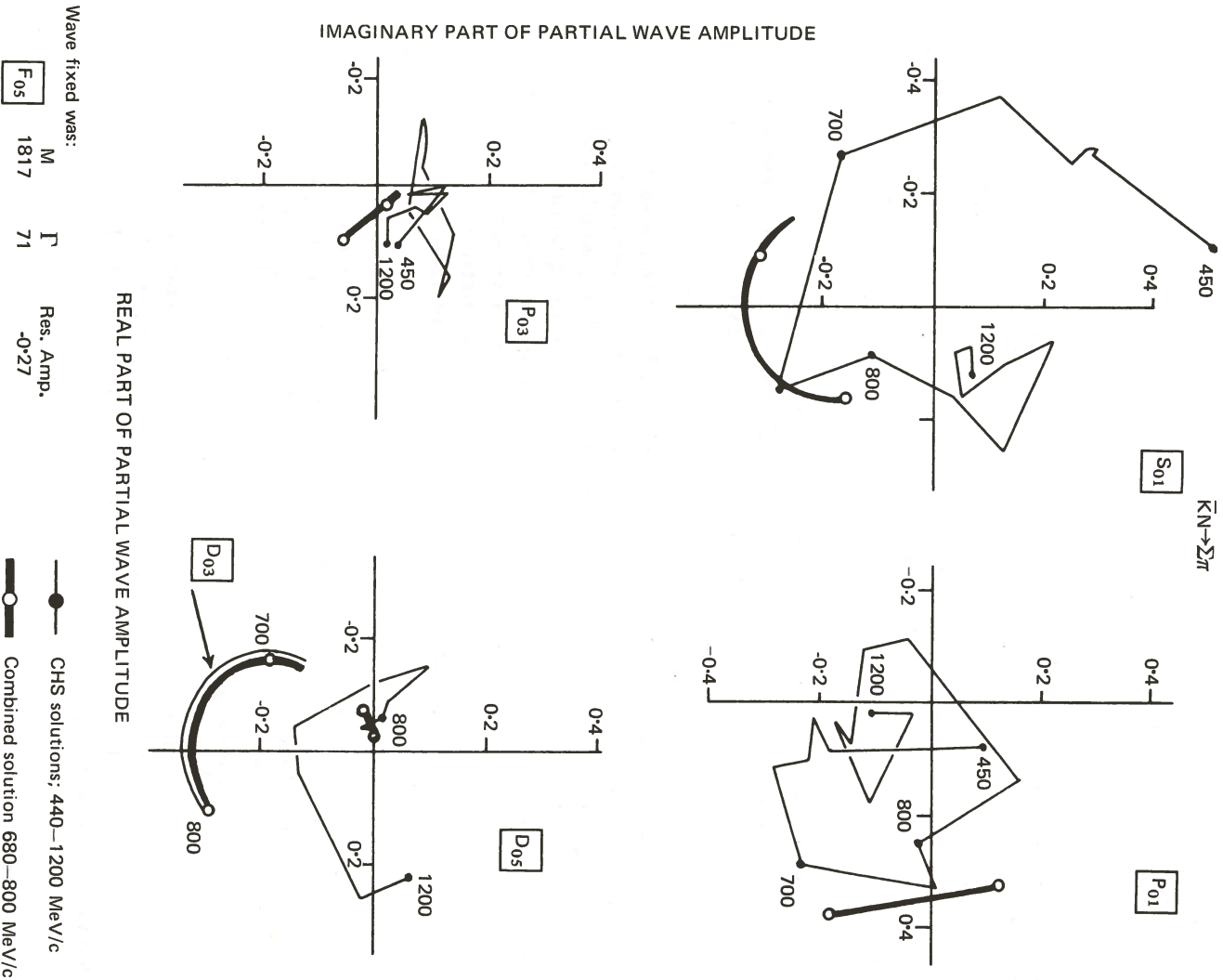
Experimentally, the unambiguous separation of these states, and others like $\Lambda\pi^0\pi^0$, depends on high gamma ray detection efficiency, for it is essential to observe all the gamma rays from the decay of the neutral pions. In this experiment the high efficiency is achieved by surrounding the liquid hydrogen target as completely as possible with steel plate spark chambers. In these the gamma rays have an individual probability of 98% of converting into a visible electron-positron shower. A scintillation counter system rejects those events which do not correspond to an 'all neutral' final state, from which a later Λ decay produces charged particles. These charged particles are also detected, both in magnetostriptive wire spark chambers which lie between the hydrogen target and the gamma chambers, and in the gamma chambers themselves.

Selection of events is initially made by scanning and then by kinematic fitting. A total of $\sim 3,500 \Lambda \pi^0$ events and $\sim 1,600 \Sigma^0 \pi^0$ events is expected when analysis is complete.

Data was taken at 16 momentum values between 685 MeV/c and 990 MeV/c, and some data has been analysed to obtain preliminary $\Lambda \pi^0$ and $\Sigma^0 \pi^0$ angular distributions for momenta between 685 MeV/c and 800 MeV/c.

A partial wave analysis has been carried out on this data combining our new data with that of the CERN Heidelberg Saclay collaboration (CHS) in the same region. Figure 13 shows the solution for the $\Sigma^0 \pi^0$ channel. The lighter lines on the amplitude diagrams are the energy independent solution of CHS, shown for the full range 440 to 1200 MeV/c, and the heavy lines are our combined solution for the range 680 to 800 MeV/c. The overall fit is reasonable, χ^2 of 100 on 87 points, though our data requires larger couplings for the $\Lambda(1670)S_{01}$ and $\Lambda(1750)P_{01}$ states, while the D_{03} state remains unchanged.

Figure 13. Solution for the $\bar{K}N \rightarrow \Sigma^0 \pi^0$ channel obtained from a partial wave analysis of the data from Experiment 3 combined with data from the CERN/Heidelberg/Saclay collaboration.



Experiment 4

UNIVERSITY OF OXFORD
RUTHERFORD LABORATORY

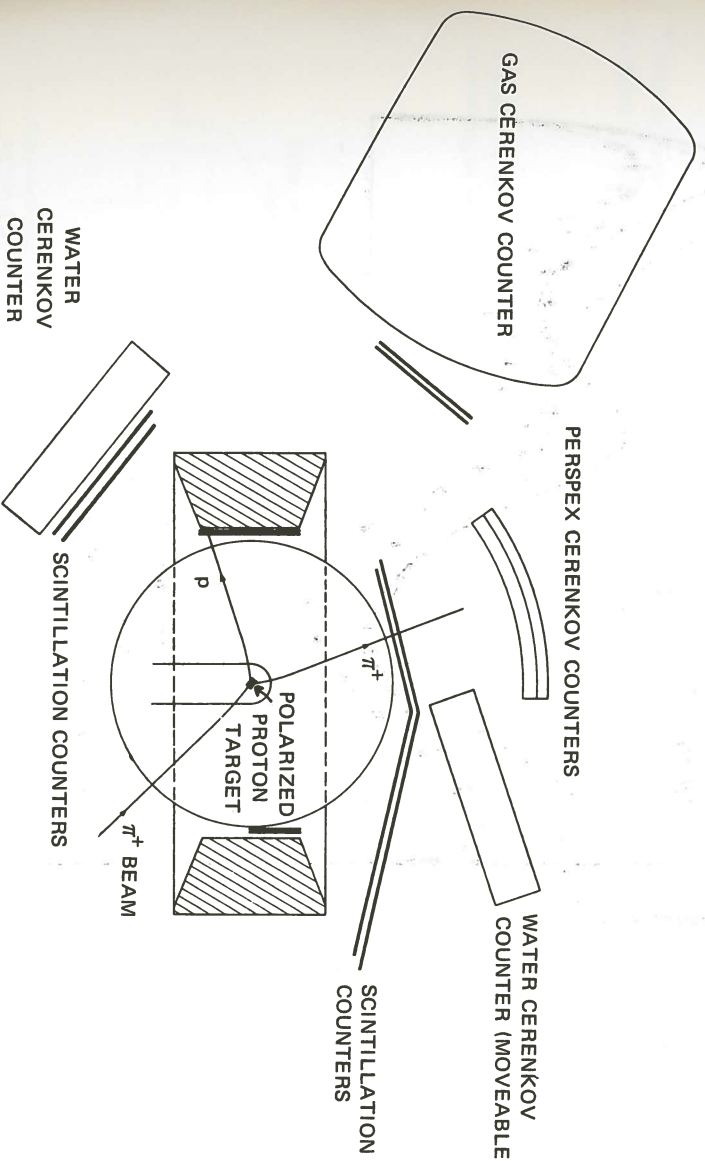
In this experiment the asymmetry in the elastic scattering of pions by polarized protons has been measured as a function of the centre of momentum angle at 68 lab. momenta between 600 and 2700 MeV/c. A large number of pion-nucleon resonances are known to be produced in this momentum range and others have been suggested by current theoretical models. One of the objects of the experiment was to provide new data to incorporate into an analysis in terms of partial wave amplitudes or phase shifts; from the behaviour of these phase shifts as a function of the momentum of the incident pion it is possible to obtain information on the properties of any resonant states which may be formed in the scattering process.

The experimental arrangement is shown in figure 14. The target consisted of an assembly of Lanthanum Magnesium Nitrate crystals, in which the free protons in the water of crystallisation were polarized by means of the 'solid effect'. The polarization, which reached values in excess of 70% during the experiment, was continuously monitored by a nuclear magnetic resonance system to an accuracy of $\pm 4\%$. The target contained approximately 16 times as many bound protons as free protons and these were not polarized.

Scattered particles were detected in hodoscopes which consisted of vertical and horizontal scintillation counters. They defined the scattering angles to within $\pm 3^\circ$ over most of the angular range, so enabling elastic events to be distinguished from the large number of background events produced, in particular, by the bound protons in the target material.

Water and perspex Cerenkov counters were used to separate pions from protons in the region where they were not clearly distinguishable by kinematics; a gas Cerenkov counter was used to reject the high background of inelastic pions which contaminated the forward scattered protons. Information from the counters was recorded on magnetic tape by a DDP 516 computer, which was also used for diagnostic purposes.

Figure 14. Schematic diagram of the apparatus used in Experiment 4 to study π^+ scattering on polarized protons.



*Polarization
Effects in π^+p
Elastic Scattering
(ref. 101)*

Experiment 5

QUEEN MARY COLLEGE, LONDON.
UNIVERSITY OF BERGEN
AERE, HARWELL
RUTHERFORD LABORATORY

Wide Angle Elastic
pp Scattering

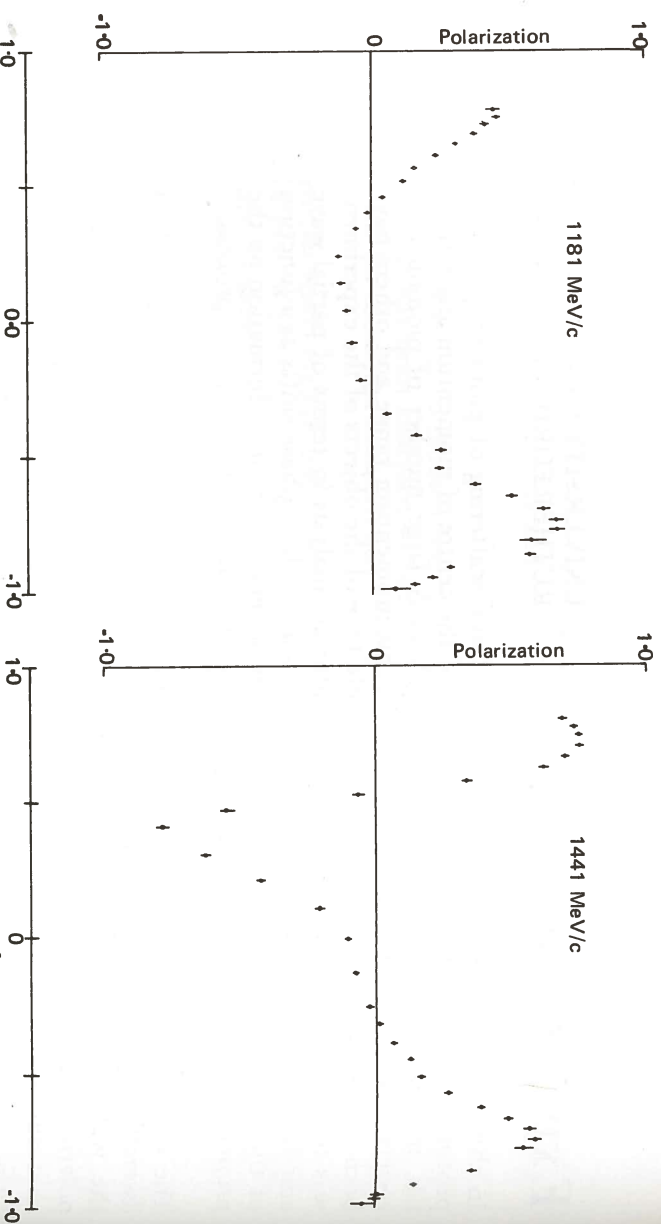


Figure 15. Results of polarization measurements at two momenta from Experiment 4. θ^* is the centre of momentum scattering angle.

The experiment was completed in November 1970. A substantial fraction of the data has undergone preliminary analysis, and the results at two momenta are shown in figure 15. Some of the data have been compared with the results of various phase shift analyses. A typical example is shown in figure 16. A search for new and better solutions will be made when the final analysis of the data is complete. However, it is already clear that the polarization is a very sensitive function of the phase shifts in this momentum region and that the results of this experiment should substantially reduce the range of values that they can assume.

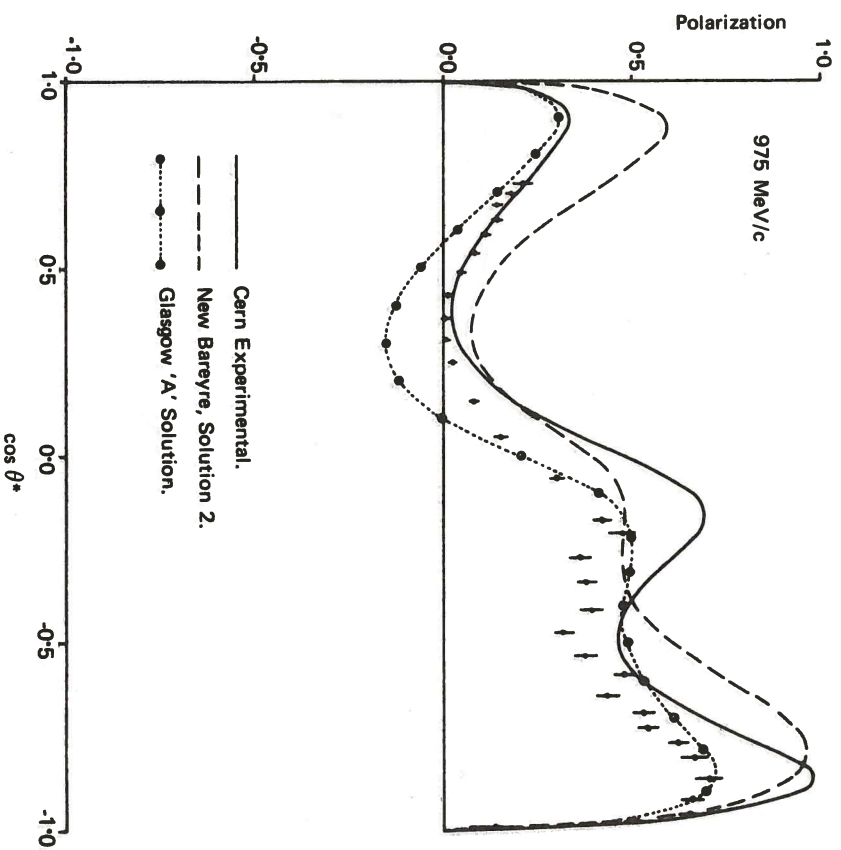


Figure 16. Polarization data at 975 MeV/c from Experiment 4 compared with some phase shift predictions.

This experiment is a measurement of differential cross-sections for proton-proton elastic scattering at lab. momenta in the range 1.3 to 3.6 GeV/c and at large cm angles (40° to 90°). Previous experiments have shown a sudden change of slope in the angular distributions when the data is presented graphically in the form log $(d\sigma/dt)$ against t . It was therefore decided to make detailed studies with high statistics using a scattered proton beam from Nimrod. Figure 17 shows a schematic diagram of the apparatus used. Protons in the P71 beam line were identified using a DISC Cerenkov counter and were elastically scattered in a 10 cm long liquid hydrogen target. Two arrays of scintillation counters detected the presence of the two outgoing protons. The electronics were set up so that only certain combinations of left and right counters gave a trigger. This lowered contamination by unwanted background processes, since many of these had the wrong angular correlation.

Three arrays of core read-out wire spark chambers recorded the trajectories of the interacting particles. An on-line PDP8 computer wrote the spark co-ordinates on to 7-track magnetic tape and also performed a series of histogramming tasks aimed at monitoring the performance of the apparatus.

Data was taken at 14 momenta and 1.25 million triggers were written on to tapes. A single program package scanned the data tapes, fitted vectors to the spark co-ordinates and wrote the parameters of possible elastic scatters on to a summary tape. A second program package scanned the summary tapes applying cuts to the candidates and calculating cross-sections from those found to be elastic events. These raw cross-sections were then corrected for any background still contained in the sample, and also for inefficiencies in spark chamber performance.

Figure 18 shows a plot of the differential cross-section versus centre of momentum angle for beam momenta of 1.7 and 3.0 GeV/c. A few corrections remain to be made but these are unlikely to exceed 5%. All the cross-sections are smoothly falling and flatten at 90° as required by particle identity. No trace of the structure seen at higher momenta in plots of $d\sigma/dt$ versus $-t$ is present.

There is some evidence for structure in the 90° cross-section (figure 19) which can be seen by plotting $d\sigma/dt$ versus $-t$ at 90° data only.

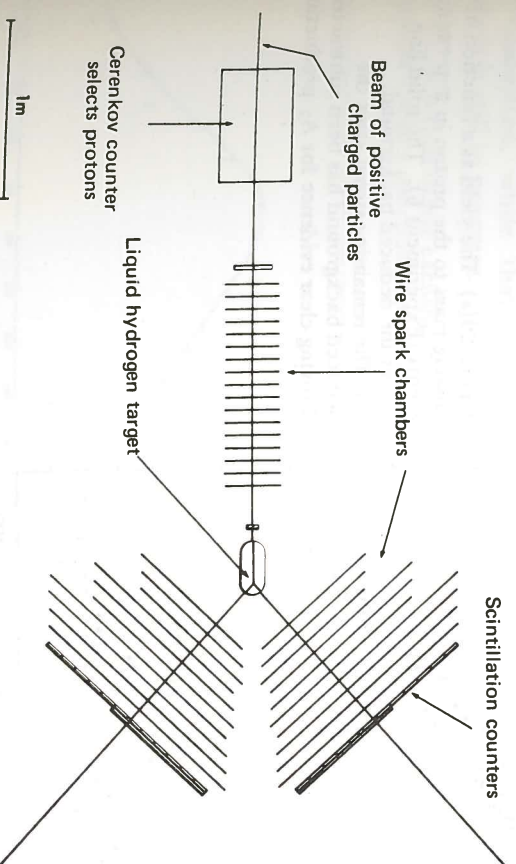


Figure 17. Schematic diagram of the apparatus used in Experiment 5 to study *pp* elastic scattering at large angles.

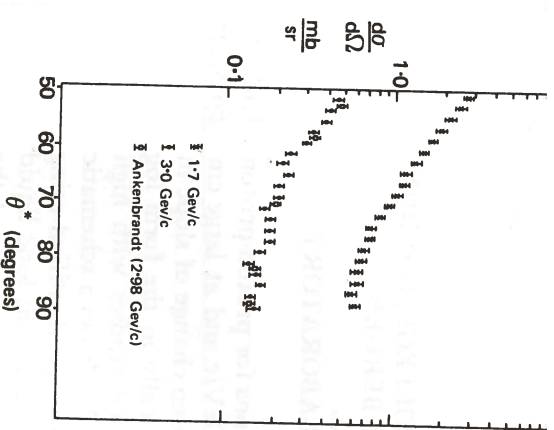


Figure 18. Differential cross-sections for pp elastic scattering versus centre of momentum angle. The points at 1.7 and 3.0 GeV/c are from Experiment 5.

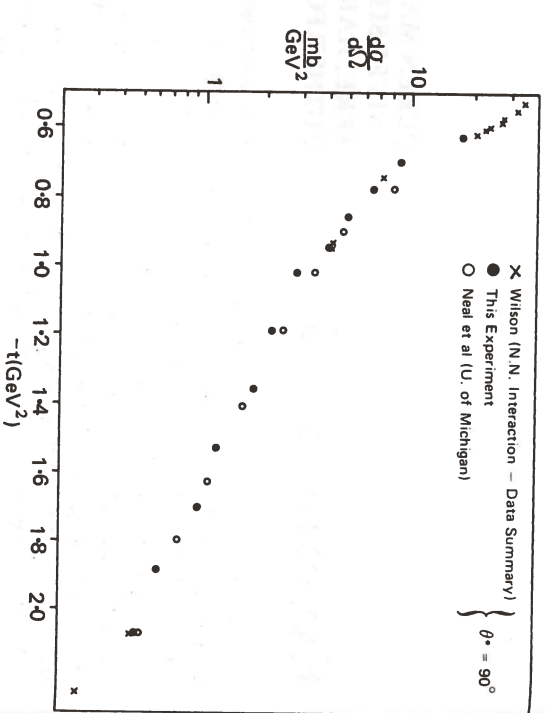


Figure 19. pp differential cross-sections at 90° centre of momentum angle versus $-t$ (four-momentum transfer squared) (Experiment 5).

Experiment 6

IMPERIAL COLLEGE, LONDON
UNIVERSITY OF SOUTHAMPTON

An Investigation of Narrow Width Mesons Produced in π^-p Interactions (ref. 138)

This is a 'missing mass' type of experiment, in which the yield of neutrons and protons from π^-p interactions is studied as a function of the incident pion momentum. When the direction and momentum of the outgoing nucleon are known, the mass of the recoiling system (the 'missing mass') can be directly calculated, using kinematical constraints of energy and momentum conservation. The intention in this experiment is to search for, and study, narrow mesons in the mass range 500 to 2000 MeV/c².

The equipment consists essentially of a precisely controlled and variable momentum pion beam, a hydrogen target, six neutron counters near the forward direction and, surrounding the target, an arrangement of counters differentially sensitive to both charged particles and photons. Such an all-counter system permits very high data rates, compared with experiments incorporating spark chambers, but relatively little rejection of spurious events is possible once the data has been recorded.

One of the problems in all missing mass experiments is the background signal which has to be subtracted. Analysis procedures have been devised to enable this to be done reliably. As an example, the yield as a function of missing mass to the proton in $\pi^+\pi^-\pi^+p$ final states is shown in figure 20a together with the estimated background. Figure 20b shows the subtracted signal, with clear evidence for A_2 production.

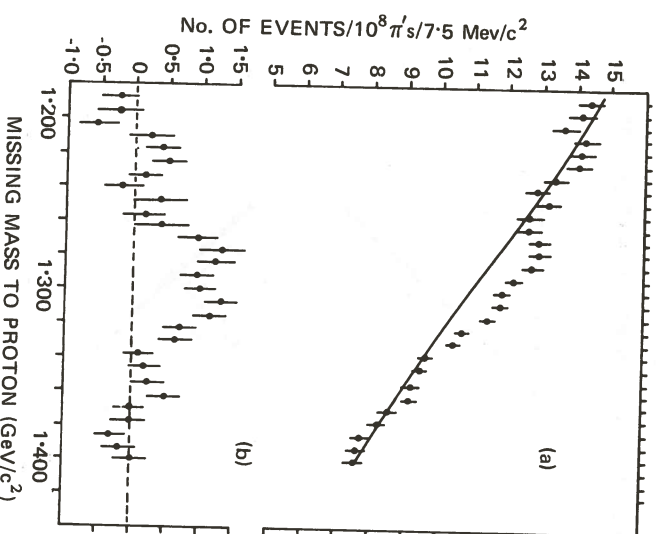


Figure 20(a) The yield as a function of missing mass to the proton in $\pi^+\pi^-\pi^+p$ events (Experiment 6). The solid line shows the deduced background. (b) The remaining signal after the deduced background has been subtracted showing clear evidence for A_2 production.

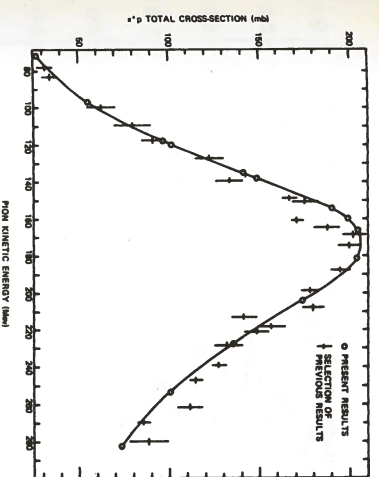


Figure 21. π^+p total cross-sections from Experiment 7 with a selection of previous results.

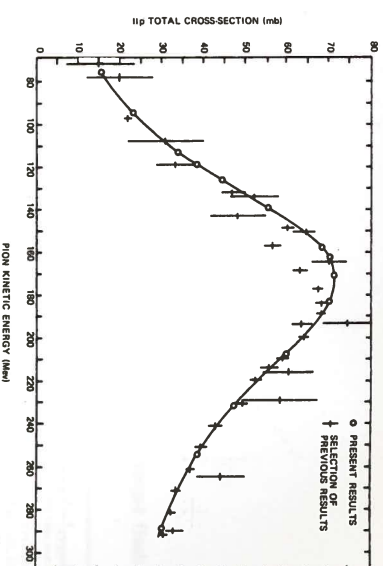


Figure 22. π^-p total cross-sections from Experiment 7 with a selection of previous results.

Experiment 7

UNIVERSITY OF CAMBRIDGE
RUTHERFORD LABORATORY

A knowledge of πN interactions in the region around the first Δ resonance is fundamental to a general study of meson-nucleon physics at higher energies. The available data were sparse and relatively inaccurate, such as to warrant a comprehensive series of measurements of total cross-sections (at the 1% level of accuracy) and angular distributions (at the 1% level of accuracy) over the energy region 80 to 300 MeV.

The experiment, carried out at the CERN Synchro-Cyclotron, completed data-taking during the summer of 1970. The total cross-sections were measured by the conventional transmission counter technique, and the charge exchange total cross-section by surrounding a liquid hydrogen target with a box of scintillators. The elastic scattering angular distributions were measured by the correlation method in the angular range where both the proton and the pion emerged from the target and otherwise by an analysis with a spectrometer magnet and sonic spark chambers, of the scattered pion only.

The results so far published include the π^+p and π^-p total cross-sections, shown in figures 21 and 22 and the $\pi^-p \rightarrow \pi^0n$ total charge exchange cross-section given in figure 23.

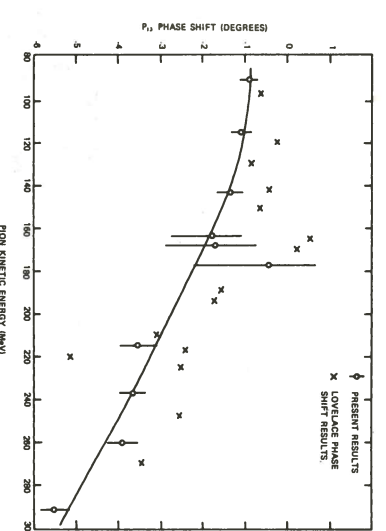
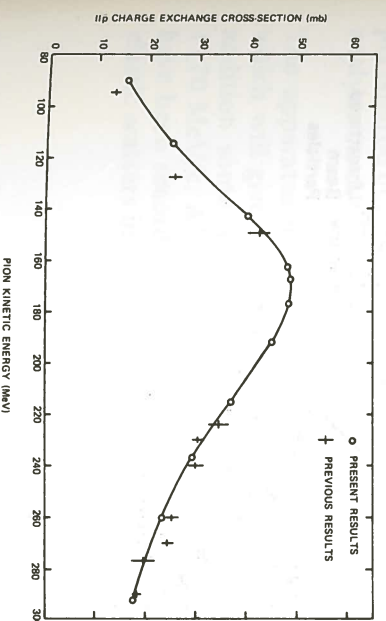
The P_{33} phase-shift has been evaluated separately for both π^+p and π^-p states. By removing the 'inner Coulomb' effects (neglected in previous analyses) parameters have been obtained for the Δ resonance in both the neutral and doubly charged states. The mean mass is 1231.7 MeV/c², with a $\Delta^0 - \Delta^{++}$ mass difference of ≈ 2.9 MeV/c². The same elastic width of 113 MeV/c² is observed in both states, indicating the isospin invariance of the pion-nucleon coupling constant.

The P_{13} phase-shift shown in figure 24 has been calculated from the π^-p total cross-section and the $\pi^-p \rightarrow \pi^0n$ total cross-section.

The analysis of the angular distribution data taken in the correlation mode has been completed, while that using the spectrometer magnet and sonic spark chambers is still in progress.

Figure 23. π^-p total charge exchange cross-section from Experiment 7 with a selection of previous results.

Figure 24. The P_{13} phase shift calculated from the π^-p total cross-sections and the $\pi^-p \rightarrow \pi^0n$ total cross-sections measured in Experiment 7.



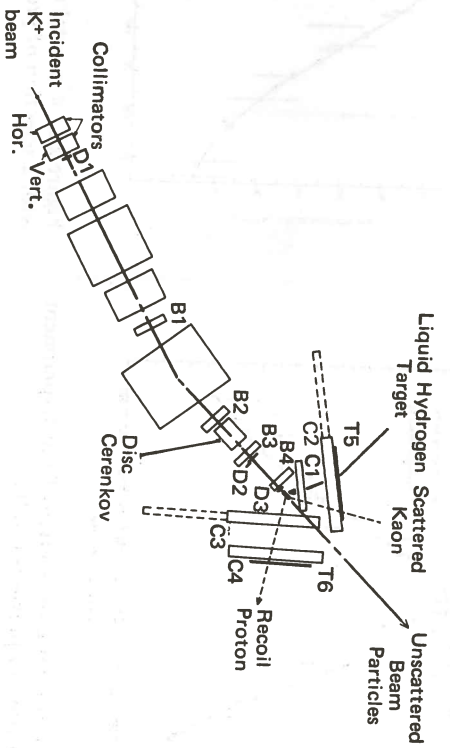


Figure 25. Schematic diagram of the apparatus used in the correlation mode of Experiment 8 to study K^+p scattering. D1 to D3 are scintillation counters and T5 and T6 are arrays of similar counters. B1 to B4 and C1 to C4 are sonic spark chambers.

Experiment 8

UNIVERSITY OF BRISTOL
RUTHERFORD LABORATORY

K^+p Differential Cross-Sections in the Range 0.9 to 2.0 GeV/c

The scattering by nucleons of positive kaons differs from that of other mesons in that resonant states are produced either very weakly, or not at all! This fact agrees well with the quark model; the composite states (π^+p), (π^-p) or (K^-p) have quantum numbers which could be made up by combining just three quarks (qqq) whereas the state (K^+p) cannot be obtained from three quarks, but would require a five quark combination (qqqqq). In the simplest quark model it is postulated that these more complex states either do not exist or are produced relatively weakly. These facts have made K^+p scattering of especial interest, first to confirm whether there is in fact a small amount of resonance-like behaviour, and second to study other mechanisms of scattering in a situation where they are not dominated by resonance scattering.

The purpose of this experiment is to measure differential cross-sections for K^+p elastic scattering which, with polarization measurements from other experiments, provide a basis for a detailed phase-shift analysis of the K^+p interactions.

The Nimrod extracted proton beam X3 strikes a 10 cm copper target to produce a secondary beam of positive kaons with a momentum which can be varied from 900 to 2000 MeV/c. This passes through two stages of electrostatic separation to remove unwanted pions and protons. The kaon beam is focused on a 30 cm liquid hydrogen target after passing through a series of beam defining counters (D₁, D₂ and D₃, see figure 25) and a DISC differential Cerenkov counter which gives positive identification of kaons. There are also four acoustic spark chambers (B₁, B₂, B₃ and B₄ in figure 25) which are situated in the beam in front of the target. Of these the combination B₁ B₂ B₃ serves to determine the momentum of the beam particle from the angle of bend in the magnet M205 while the combination B₃ B₄ gives the angle at which the kaon enters the target.

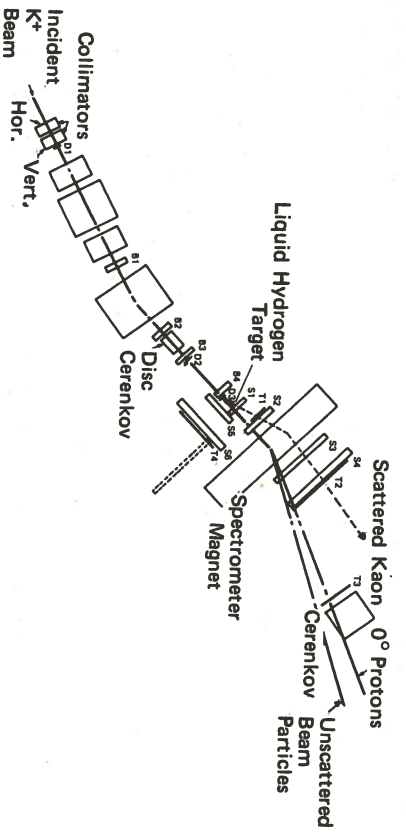


Figure 26. Schematic diagram of the apparatus used in the spectrometer mode of Experiment 8. D1 to D3 are scintillation counters, and T1 to T4 arrays of similar counters. B1 to B4 and S1 to S6 are sonic spark chambers.

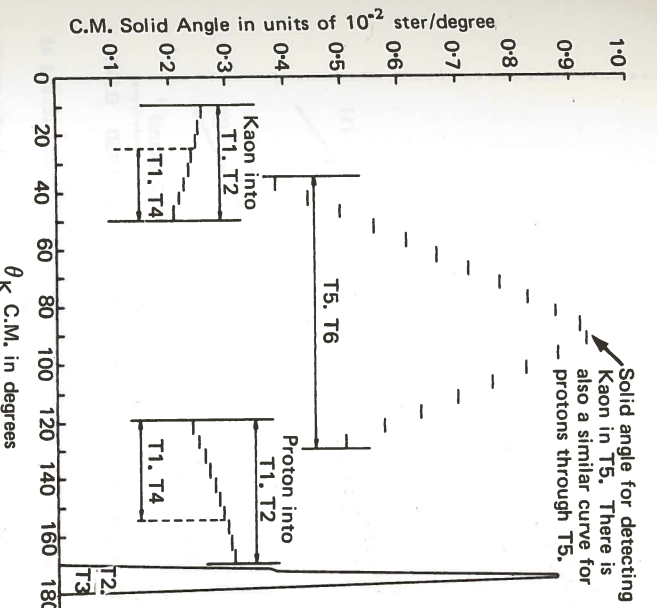


Figure 27. The solid angle for particle detection obtained with different trigger conditions for a K^+ beam momentum of 1 GeV/c (Experiment 8).

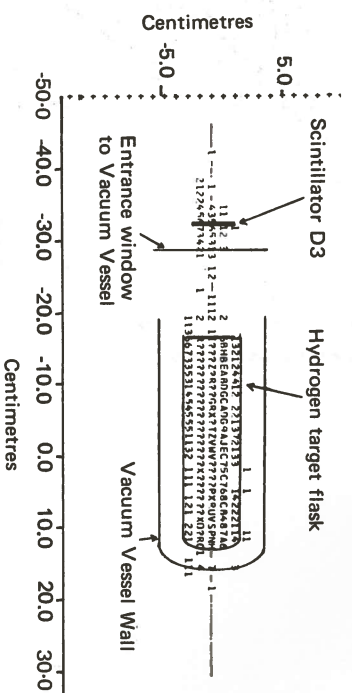


Figure 28. Scatter plot showing the distribution of scattering vertices in the region of the hydrogen target. The number of times vertices occur at the various points are indicated by incrementing through 1 to 9 then A to Z while symbol ? indicates greater than 35. (Experiment 8).

The elastic scattering events are detected in two alternative sets of acoustic spark chambers, each with its appropriate trigger counters which provide the signal to fire the spark chambers. Figure 25 shows the correlation system which identifies elastic K^+p scattering by observing the angles with respect to the incident kaon of both the scattered kaon and recoil proton; this covers a range of laboratory angles from 17° to 80° , the trigger condition being one particle through the trigger counter array T5 in coincidence with one through T6 (i.e. T5 + T6).

Figure 26 shows the 'spectrometer' mode which covers those angles where one particle may not have sufficient energy to escape from the target. The identification of elastic events is obtained by measuring the scattering angle and momentum of one particle. The spark chambers S₁ and S₂ give the scattering angle, while S₃ and S₄ give the momentum from the bend in the magnet M505/M506.

The spectrometer system covers a range of scattering angles from 3° to 25° in the laboratory reference frame; for the upper part of this range, the recoil particle has sufficient energy to be detected in the chambers S₅ and S₆. This provides some data which may be analysed either as 'spectrometer' or 'correlation' mode, giving a valuable check on the analysis. The trigger combinations for the above are T1 + T2 or T1 + T4. A third combination of trigger arrays, T2 + T3, examines the case of scattering near 180° which gives a recoil proton near 0° with momentum considerably higher than that of the incident kaon. The large threshold Cerenkov counter behind the array T3 serves to reduce the trigger rate from the decay of unscattered beam kaons. The solid angle for particle detection in the different trigger conditions is shown in figure 27.

Digital information of the positions of tracks in the spark chambers is fed, along with readings of scalars and trigger counter registers, into the core of an on-line Ferranti Argus 400 computer, which stores details of up to ten scattering events per Nimrod burst, checking the first and copying all on to magnetic tape for further analysis on the IBM 360 computer.

The apparatus has now been set up and tests with a pion beam have been made which will give π^+p differential cross-sections having value in their own right. In addition some K^+p data has been taken at momenta of 1615, 1465, 1300 and 1170 MeV/c. A total of 130,000 events (including about 48,000 elastic scatters) have been recorded in the correlation mode and 300,000 events including 10,000 elastic scatters in the spectrometer mode.

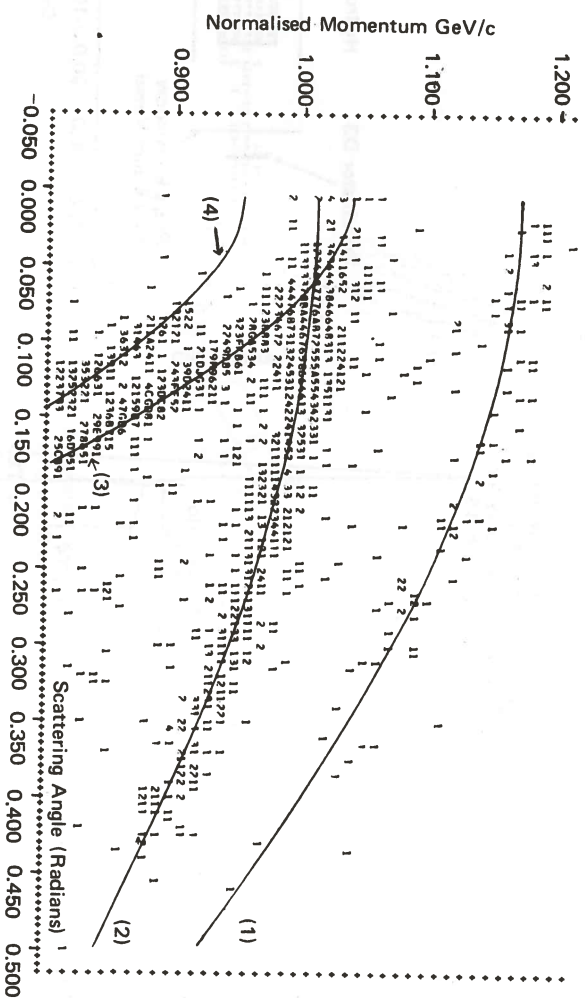


Figure 29. Scatter plot of particle momentum against angle of emission for K^+ scattering at 1.45 GeV/c. (Experiment 8).
The solid lines on the plot are kinematical predictions:—(1) Recoil protons from elastic scattering. (2) Elastically scattered kaons. (3) Muons from the decay $K^+ \rightarrow \mu^+ \nu$. (4) pions from the decay $K^+ \rightarrow \pi^+ \pi^0$.

Preliminary analysis shows good separation of elastic events. In the correlation mode the background is completely negligible because of the tight limits which can be imposed. The accuracy of reconstruction of events is illustrated by figure 28, which shows the distribution of scattering vertices in the region of the target. In the spectrometer mode, a plot of particle momentum against angle of emission (figure 29) shows satisfactory discrimination of elastic events from the background of $K^+ \rightarrow \mu^+ \nu$ and $K^+ \rightarrow \pi^+ \pi^0$ decays.

The recoil protons from events near 180° are particularly well distinguished, and it is expected that good backward points will be a valuable feature of the final results. Analysis is proceeding.

Experiment 9

UNIVERSITY OF BIRMINGHAM
RUTHERFORD LABORATORY

This experiment, which complements Experiment 1, is a measurement of K^+n elastic and charge exchange scattering and K^-n elastic scattering over the momentum range 0.45 to 0.95 GeV/c using a liquid deuterium target and sonic spark chambers. The K^+n scattering, when combined with K^+p which is a pure isotopic spin state with $I = 1$, allows the $I = 0$ state of the K -nucleon system to be studied. There is great interest in the structure in this system centred at 0.75 GeV/c, as observed in measurements of K^+p and K^+d total cross-sections made by a group at this Laboratory and more recently by an Arizona group working at Berkeley, which could be an exotic Z^* resonance. The K^-n data, on the other hand, will add to our knowledge of Y^* resonances and has the advantage of being a pure $I = 1$ state. Relatively little is known about the details of the angular distributions for any of these processes at the present time and this experiment will provide about 10^4 events for each channel at each of the momenta studied in Experiment 1.

Figure 30 shows a sketch of the apparatus which relies on identifying a K -meson by its decay in flight between chambers C3 and C4. Protons from the charge exchange process are recognised by their longer time of flight to T4 counters as well as their non-decay. Extensive tests of the equipment were carried out prior to the December shutdown and in the last few days some test data were obtained, following the first filling of the deuterium target in the beamline, with most of the apparatus working. If these data prove to be satisfactory data taking will start early in 1971.

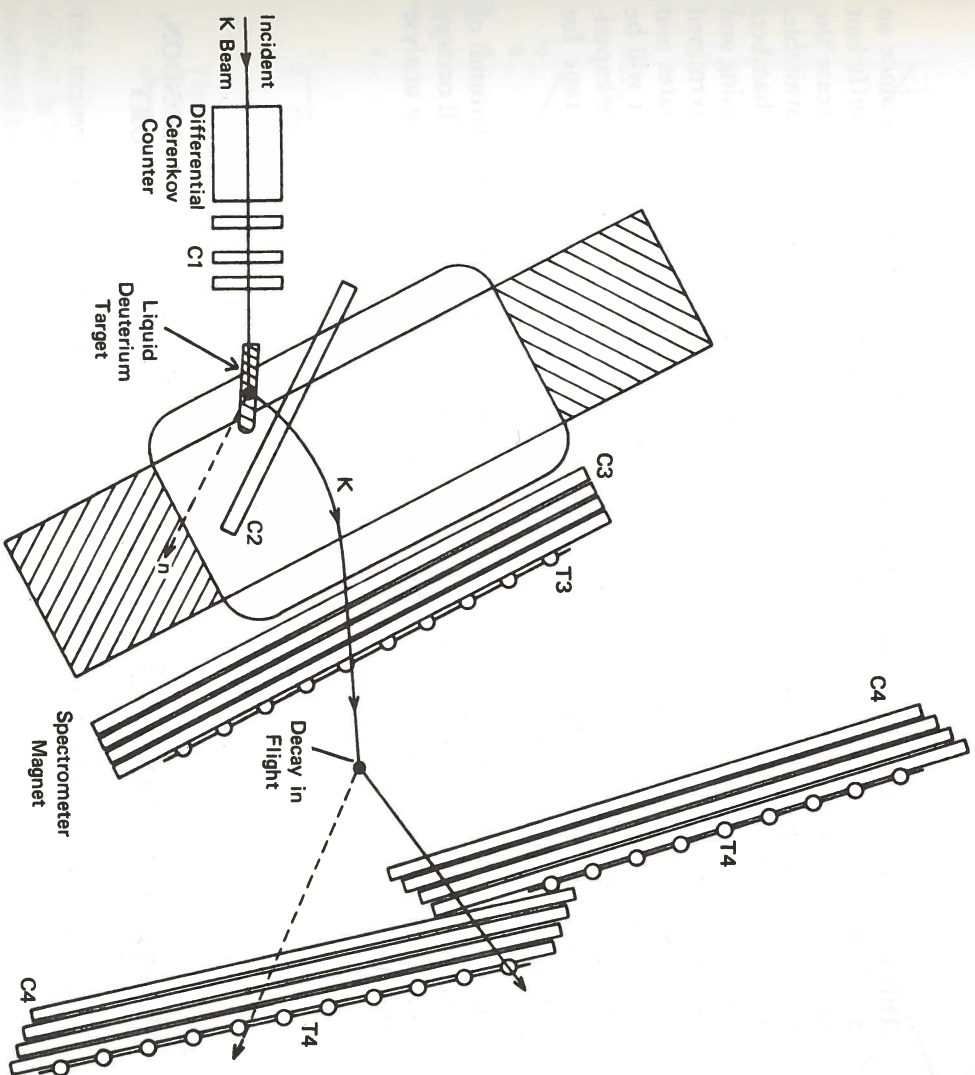
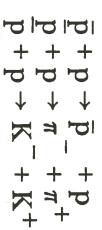


Figure 30. Schematic diagram of the apparatus used in Experiment 9 to study K^+n scattering. C1 to C4 are sonic spark chambers and T3 and T4 are counter hodoscopes. There are veto counters (not shown) around the target and in the residual beam.

Experiment 10

QUEEN MARY COLLEGE, LONDON.
UNIVERSITY OF LIVERPOOL
DARESBUURY LABORATORY
RUTHERFORD LABORATORY

Some meson resonances have masses greater than two nucleons and hence may decay into a proton-antiproton pair as well as into other mesons. It is possible therefore to study such heavy mesons by means of a 'formation' experiment in which stationary protons in a hydrogen target are bombarded by an antiproton beam. The beam momentum is chosen so that the invariant mass of the $p\bar{p}$ system equals the mass of the meson being studied. By varying the beam momentum in a number of steps a range of masses can be studied. In this experiment it is proposed to run at momenta from about 0.7 to 2.0 GeV/c so that mesons having masses from about 2.0 to 2.4 GeV/c² would be studied. The apparatus is designed to investigate the reactions



which correspond to heavy mesons decaying into $\bar{p}p$, $\pi^- \pi^+$ or $K^- K^+$ by means of the strong interaction which was also responsible for their formation. By measuring the differential cross-sections of these reactions information about the angular momentum quantum numbers of heavy mesons and the coupling strengths to the $\pi^- \pi^+$ or $K^- K^+$ states can be obtained.

*Antiproton-Proton
Elastic Scattering
and Two Body
Annihilation*

This experiment is being conducted at the CERN Proton Synchrotron since an accelerator having a higher energy than Nimrod is required to produce a sufficient flux of antiprotons. A new beamline has been designed which will increase the number of antiprotons in the required energy range over that previously available, and this will be set up at the beginning of 1971. Counters and wire spark chambers with ferrite core read-out will be used to detect the positions of the incoming and outgoing particles, and the momentum of one outgoing particle will be determined by passing it through a large spectrometer magnet. The spark co-ordinates and information from the counters and other components of the experiment will be read into a PDP 9/L computer, which will provide an on-line monitor of the experiment and also record data from each scattering event on to magnetic tape for subsequent full analysis by a large computer.

Most members of the experimental group moved to CERN during the Autumn of 1970. It is expected that the setting up and running of the experiment will occupy the whole of 1971 and that the group will return to the UK in 1972 to analyse the data.

Experiment 11

QUEEN MARY COLLEGE, LONDON.
RUTHERFORD LABORATORY

The sigma minus decay:



A Measurement of the
Electron Asymmetry
Parameter in the Decay
of Polarized Σ^-
(ref. 130)

is a weak interaction, and is classified to be of the semi-leptonic type. That is, it involves two leptons and two hadrons (strongly interacting particles). The presence of the strong interactions is known to produce important corrections to the otherwise simple and rather well understood weak interaction processes. The sigma beta decay, in common with neutron beta decay, cascade beta decay, and many other semi-leptonic processes has the interesting feature that the strong interaction will upset only two out of the four particles involved in the basic weak interaction. The process is described by an interaction Hamiltonian:

$$H = J_W^{\text{Hadrons}} \times J_W^{\text{Leptons}}$$

i.e. a product of two 'currents', J_W^{Leptons} is a weak interaction 'current' involving the two leptons, similarly J_W^{Hadrons} acts between the two hadrons and is therefore perturbed by the strong interaction.

N. Cabibbo has invented a most interesting theory in which the currents J_W^{Hadrons} for all possible Hadron pairs are algebraically related by way of SU(3) theory. This means in practice that the behaviour of all semi-leptonic processes can be inter-related through SU(3) algebra and its Clebsch-Gordon coefficients. Thus if the physical behaviour of a few processes is known, it is possible to make predictions about many other processes. One of the key tests of the Cabibbo theory is to study the asymmetry in the Σ^- beta decay. The prediction, using data from other leptonic processes, is that a weak interaction admixture of the form $V + 0.3A$ will apply, in dramatic contradiction to simpler theories which give the standard $V-A$ form for the weak interaction process, where V refers to vector interaction and A refers to axial-vector interaction.

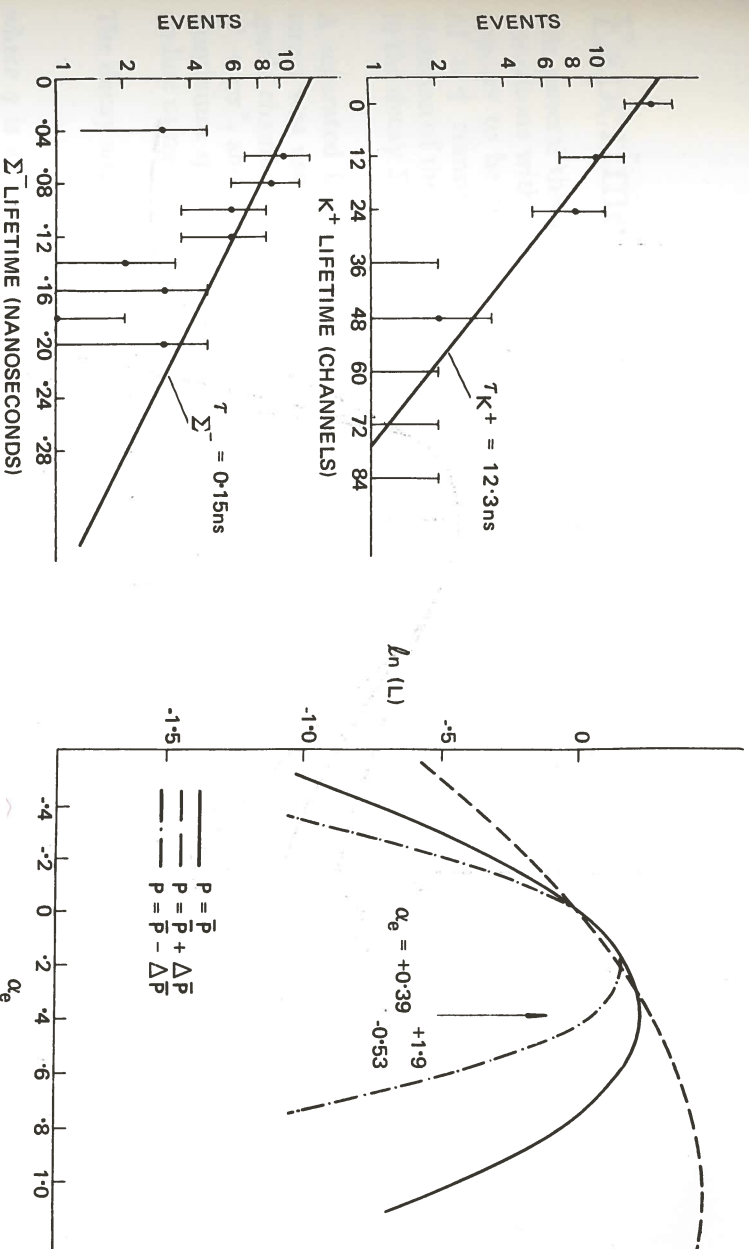


Figure 31. K^+ and Σ^- lifetime spectra determined in the Σ^- beta-decay experiment (Experiment 11).

Figure 32. The logarithm of the likelihood function plotted against the electron asymmetry parameter α_e . (Experiment 11).

The experiment has now been completed. The experimental method has been described in earlier Annual Reports. Some normal Σ^- decay data were recorded and analysed to provide a check of the method and apparatus. 857 normal decay events were analysed. The K^+ and Σ^- lifetime spectra are shown in figure 31. Fits to these spectra, which are shown in table 10, give lifetimes in agreement with previously measured values and indicate that no background is present.

Table 10

	K^+		Σ^-	
	Lifetime nano-seconds	Background Events per 6 nano-seconds	Lifetime nano-seconds	Background Events per 0.05 nano-seconds
Normal Decay	13.7 ± 0.7	-1.3 ± 1.2	0.15 ± 0.01	-0.6 ± 1.5
Beta Decay	14.2 ± 4.4	0.7 ± 0.7	0.12 ± 0.10	0.3 ± 3.0
World Value	12.35 ± 0.04	—	0.149 ± 0.003	—

The same method of analysis was used for the Σ^- beta decay data, except that each event was visually scanned to remove background, e.g. electron-positron pairs from the Dalitz decay of π^0 's, which are not significant in the normal decay data. 43 Σ^- beta decay events were found. The logarithm of the likelihood function is shown plotted against the electron asymmetry parameter, α_e , in figure 32.

Three Σ^- polarization spectra were used viz. $P(\theta) = \bar{P}(\theta) - \Delta P(\theta)$, $P(\theta) = \bar{P}(\theta)$ and $P(\theta) = \bar{P}(\theta) + \Delta P(\theta)$ where $\bar{P}(\theta)$ is the measured Σ^- polarization distribution so that the statistical error on the Σ^- polarization ($\Delta P(\theta)$) is folded in. We find:

$$\alpha_e = 0.39 \pm 1.9$$

$$\alpha_e = 0.39 \pm 0.53$$

Experiment 12

WESTFIELD COLLEGE, LONDON
RUTHERFORD LABORATORY

*Test of the
ΔI = 1/2 Rule in
the Decay Σ* → pπ°*

The general theory of weak interactions allows non-leptonic strangeness changing transitions with a change in isotopic spin $\Delta I = \frac{1}{2}$, $\frac{3}{2}$ or $\frac{5}{2}$. A good experimental rule appears to be that in such transitions $\Delta I = \frac{1}{2}$ dominates. Small contributions of $\Delta I > \frac{1}{2}$ transitions are allowed by the experimental data. A sensitive test for violation of the empirical $\Delta I = \frac{1}{2}$ rule is a measurement of the so-called γ parameter in the decay $\Sigma^+ \rightarrow p\pi^0$.

A separated beam of π^+ mesons at 1.11 GeV/c incident upon a liquid hydrogen target was used to produce polarized sigmas by the reaction $\pi^+p \rightarrow \Sigma^+K^+$. Thin foil spark chambers measured the direction of the K^+ and the decay proton from $\Sigma^+ \rightarrow p\pi^0$, and the polarization and range of the proton were measured in a 60 gap aluminium spark chamber. The image of the spark chamber tracks were digitised on-line using a vidicon system.

The decay angular distribution is given by:

$$I = 1 + \alpha \hat{P}_\Sigma \cdot \hat{q}$$

where q is a unit vector along the momentum of the decay proton and \hat{P}_Σ is the polarization of the Σ^+ in the production reaction.

Figure 34. The distribution of $-\alpha P$ plotted against the centre of momentum production angle. The data from Experiment 12 is compared with existing bubble chamber data at the same momentum and the predicted polarization from phase shift solutions of all the ΣK production data up to 1170 MeV/c.

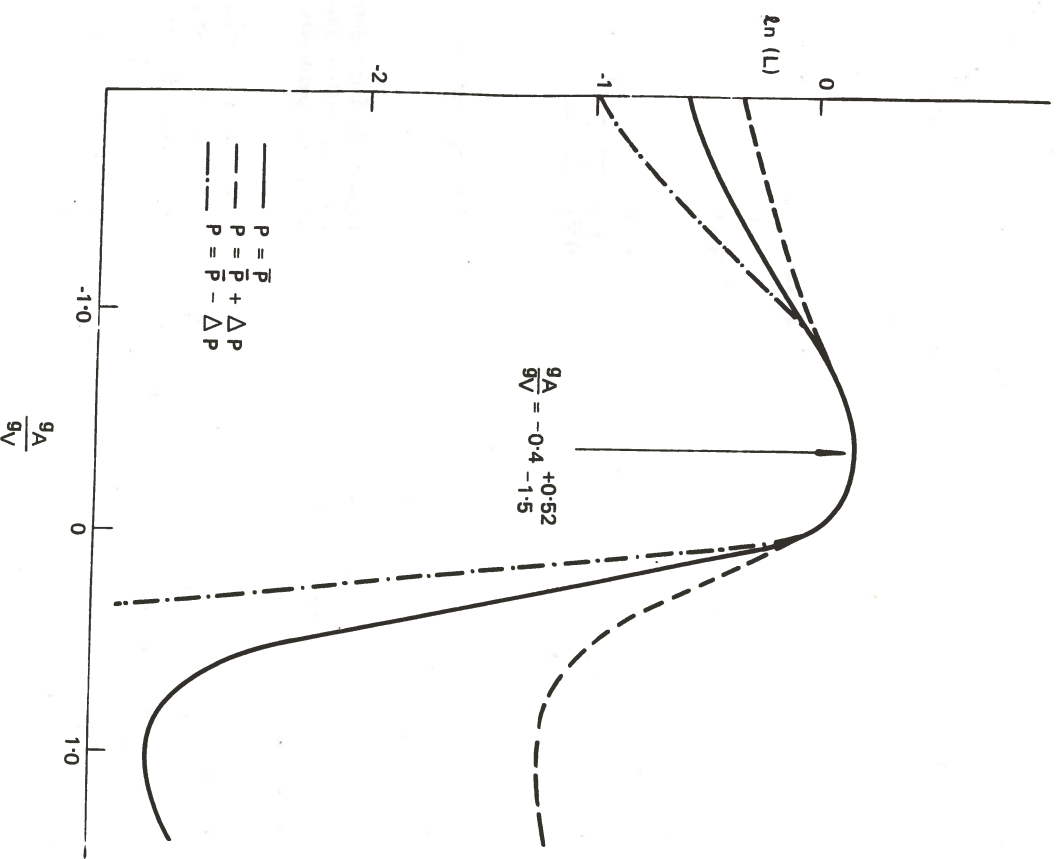
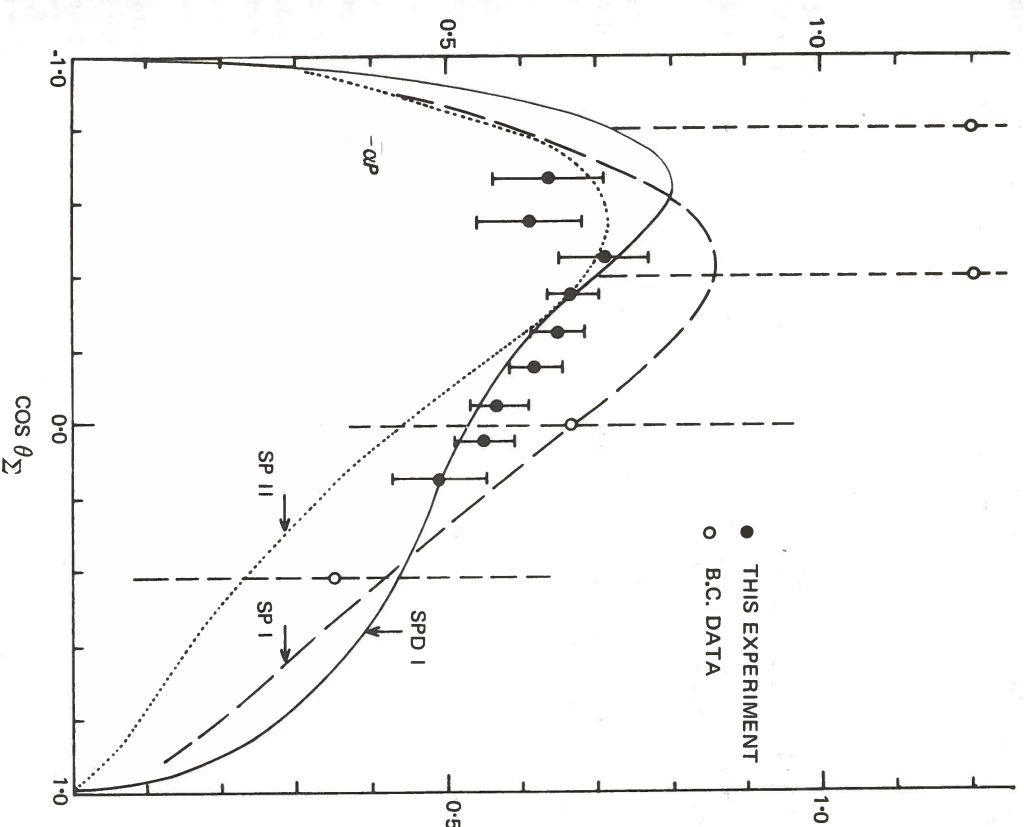


Figure 33. The logarithm of the likelihood function plotted against g_A/g_V (Experiment 11).

Figure 33 shows the logarithm of the likelihood function plotted against g_A/g_V , the coefficient of A in the weak interaction admixture, which is calculated from the asymmetry again for each of the three Σ^- polarization spectra. The ratio was found to be:

$$g_A/g_V = -0.4^{+0.52}_{-1.5}$$

that is the interaction is within the errors quoted, $V - 0.4 A$.

In Cabibbo theory the $|\Delta S| = 0$ and $|\Delta S| = 1$ weak currents are in the same SU(3) octet so that $|\Delta S| = 0$ and $|\Delta S| = 1$ decays should be fitted by the same parameter values.

From the parameters obtained by using all data other than that on g_A/g_V , one obtains a prediction for this quantity of $+0.33$. Although this disagrees with our result the discrepancy is less than two standard deviations. There are two other measurements of the sign and magnitude of g_A/g_V , which are of comparable accuracy to our own. Combining the three results one obtains two solutions of comparable probability, $g_A/g_V = \pm 0.25$ with an error of ± 0.11 . Thus, in spite of three measurements, the sign of this quantity is unresolved at the present time.

In figure 34 the distribution of $-aP$ is plotted against the centre of momentum production angle. The present data is compared with the existing bubble chamber data at this momentum and with the predicted polarization from phase shift solutions of all the ΣK production data up to 1170 MeV/c by another Nimrod group. (Experiment 2, Annual Report 1968). Since α is close to -1.0 , the experiment selects the SPD I solution in preference to the solutions SP I and SP II. The S and P wave solutions (SP.....) were found in an energy dependent search between threshold and 1130 MeV/c. The SP and D wave solution (SPD I) was found by fitting all the previous data from threshold to 1170 MeV/c.

The presence of $\Delta I \geq \frac{3}{2}$ and of time reversal violating contributions to the decay $\Sigma^+ \rightarrow p\pi^0$ can be inferred from the decay parameters α , β and γ obtained by measuring the decay proton polarization in the aluminium plate spark chamber. Since $\alpha^2 + \beta^2 + \gamma^2 = 1$ it is convenient to parameterize the decays in terms of α and the angle ϕ defined by

$$\begin{aligned}\beta &= (1 - \alpha^2)^{1/2} \sin \phi \\ \gamma &= (1 - \alpha^2)^{1/2} \cos \phi\end{aligned}$$

Several thousand scatters have been identified and these data are being investigated for systematic effects. A subset of 1,400 events in a restricted range of production angles has been analysed by the maximum likelihood method, yielding:

$$\alpha = -0.95 \pm 0.05, \quad \phi = -6^\circ \pm 45^\circ$$

When the complete sample of data is analysed an overall fit to all the charged sigma decays will be made. The present indications are that the contributions from $\Delta I \geq \frac{3}{2}$ transitions and time reversal violations are indeed small.

Experiment 13

UNIVERSITY OF CAMBRIDGE
RUTHERFORD LABORATORY

*Test of the
 $\Delta S = \Delta Q$ Rule for
 K^0 Leptonic Decays*

The present theory of weak interactions has been built up assuming several basic selection rules. Amongst these, two fundamental ones are:

a) CP Conservation (This assumes that the forces governing the weak decays are unchanged if one simultaneously changes particles into antiparticles and reflects the co-ordinate systems in a mirror).

b) $\Delta S = \Delta Q$ rule (The rule permits weak decays for which the change in strangeness of the strongly interacting particles (ΔS) is equal to the corresponding change in charge (ΔQ)).

The theory has enjoyed considerable success; violation of the two selection rules outlined above is not easily fitted into the theory. In the last few years experimental proof of CP non-conservation has been obtained for K^0 decay and, while no conclusive evidence exists for violation of the $\Delta S = \Delta Q$ rule, experiments on $K^0 \rightarrow \pi e \nu$ decay give an indication of such effects.

This experiment aims at obtaining a large sample of $K^0 \rightarrow \pi e \nu$ decays resulting from the decay of a pure K^0 state produced in the reaction $\pi^- + p \rightarrow \Lambda + K^0$. By studying the time distribution of the decaying K^0 mesons into positive and negative electrons, the amplitudes for the 'forbidden' processes $K^0 \rightarrow \pi^+ e^- \bar{\nu}$, $\bar{K}^0 \rightarrow \pi^- e^+ \nu$, for which $\Delta S = -\Delta Q$, are compared with the 'allowed' processes $K^0 \rightarrow \pi^- e^+ \nu$, $\bar{K}^0 \rightarrow \pi^+ e^- \bar{\nu}$.

The amplitude ratio is defined as:

$$x = \frac{\text{Amplitude for } \Delta S = -\Delta Q \text{ processes (forbidden)}}{\text{Amplitude for } \Delta S = \Delta Q \text{ processes (allowed)}}$$

CP conservation in the decays is checked by measuring the imaginary part of the amplitude ratio which should be zero if CP is a good symmetry for the decays.

The data analysis of the experiment is now at an advanced state. Of the 421,000 spark chamber events recorded on film, 137,000 have been completely analysed (scanned, measured, kinematically fitted and physicist scanned) giving a preliminary sample of 1,800 useful $K \rightarrow \pi e \nu$ events. Of the remaining pictures one half have been scanned and measured.

The final number of events expected (before kinematical cuts) is 5,400, half of which are carbon induced events. The expected statistical error on the amplitude ratio, x , is 3% for both the real and imaginary parts.

12,000 of an estimated total of 31,400 events recorded with a $K^0 \rightarrow \pi^+ \pi^-$ trigger have been measured on CYCLOPS and rough digitised using DMAC tables and two different interactive graphics systems.

The $K^0 \rightarrow \pi^+ \pi^-$ events will be used to check the Monte Carlo program. This program is used in the crucial task of estimating the detection efficiency of the experimental apparatus as a function of K^0 proper time. The number of events already rough digitised is sufficient for this purpose.

Studies on the preliminary data indicate that backgrounds in the $K^0 \rightarrow \pi e \nu$ event sample due to $K^0 \rightarrow \pi^+ \pi^-$, and $K^0 \rightarrow \pi^0 e^+ e^- \gamma$ decays are at an acceptably low level. A preliminary value for the amplitude ratio, x , will be published as soon as all systematic effects have been evaluated.

Experiment 14

UNIVERSITY OF GLASGOW
UNIVERSITY OF LIVERPOOL
UNIVERSITY OF OXFORD
UNIVERSITY OF WARWICK
RUTHERFORD LABORATORY

The aims of this experiment are:

(i) To measure the charge asymmetry in the rates for $K^\pm \rightarrow \pi^\pm \pi^0 \gamma$ in order to test for C non-invariance in electromagnetic interactions and CP non-invariance in the weak interaction, and also to measure for this mode the electric and magnetic dipole structure amplitudes and the interference between the electric dipole amplitude and the inner bremsstrahlung.

(ii) To measure the charge asymmetry in the rates for $K^\pm \rightarrow \pi^\pm \pi^0 \pi^0$ (τ' decay) in order to test for $I=\frac{3}{2}$, $\frac{7}{2}$ CP non-invariant terms in the non-leptonic weak interaction.

The experiment was carried out in a 5 GeV/c unseparated kaon beam at the CERN PS. A differential gas Cerenkov counter identified the kaons in the beam, and a system of counter hodoscopes and wire spark chambers at B_1 , B_2 and B_3 defined their momenta and directions. The layout of the experiment is shown in figure 35. The vector momentum of the charged pion, produced when a kaon decayed into either of the two desired final states, was measured by 12 sonic spark chambers at S_1 and S_2 in conjunction with a large spectrometer magnet. As shown in figure 35, six of these chambers were placed within the gap of the spectrometer magnet.

*A Study of the
Decay Modes
 $K^\pm \rightarrow \pi^\pm \pi^0 \gamma$
and $K^\pm \rightarrow \pi^\pm \pi^0 \pi^0$
(ref. 92, 102)*

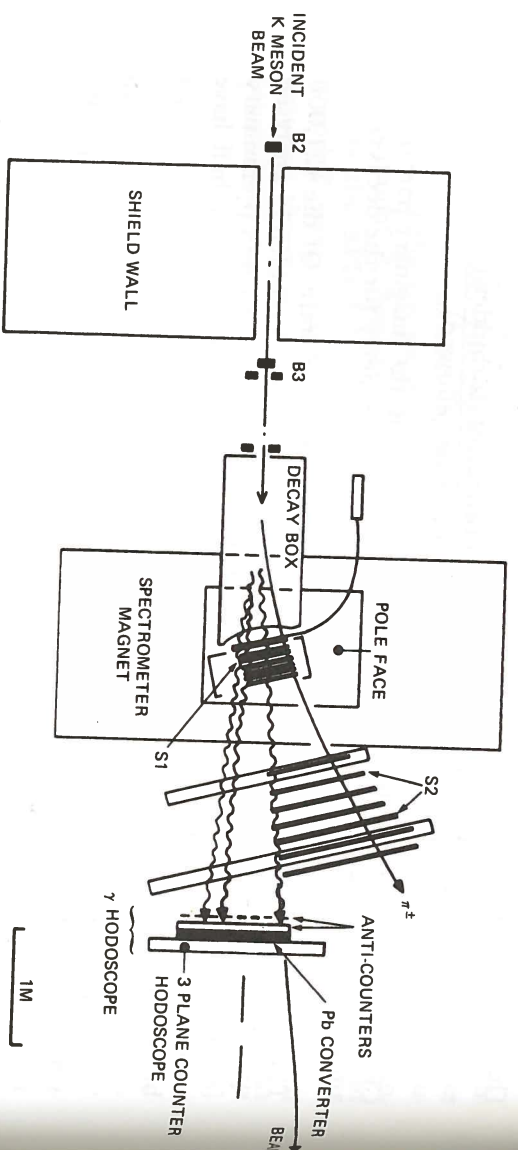


Figure 35. Schematic diagram of the apparatus used in Experiment 14 to study $K^{\pm} \rightarrow \pi^{\pm} \pi^0 \gamma$ and $K^{\pm} \rightarrow \pi^{\pm} \pi^0 \pi^0$.

Figure 36. The distribution of $A_{\tau'}$, the asymmetry parameter for the decays $K^{\pm} \rightarrow \pi^{\pm} \pi^0 \pi^0$, for 49 independent samples of data from Experiment 14.

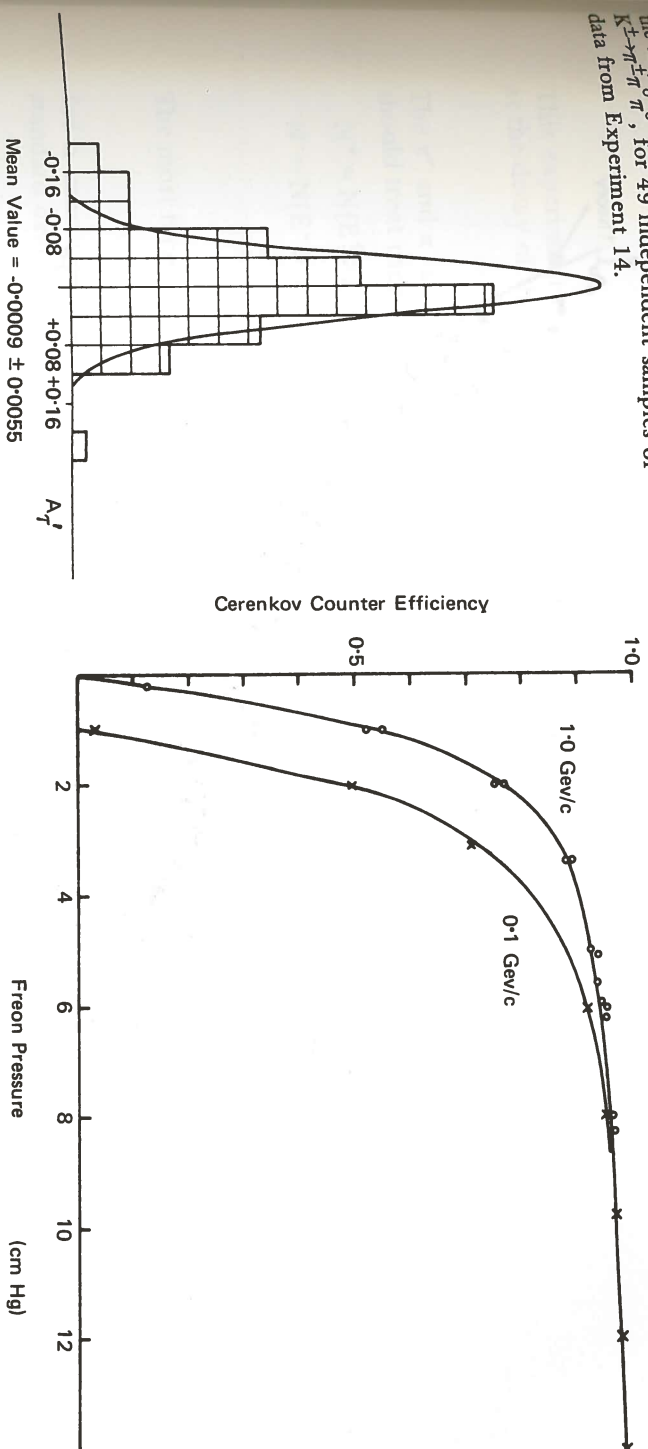


Figure 37. Efficiency of the gas Cerenkov counter as a function of gas pressure, (Experiment 15).

The final state γ -rays (including those from the decay of the neutral pions) were detected by a 1 metre square counter hodoscope. This enabled the outgoing directions of the γ -rays to be defined to within $\pm 0.5^\circ$ in the laboratory system.

Information from the counters and spark chambers was fed into a DDP 516 computer for preliminary analysis and also recorded on magnetic tape for detailed analysis. Data collection was completed in September 1969 and the results are now being analysed at the Rutherford Laboratory using the IBM 360/75.

About 30% of the data has been analysed for τ' events and about 220,000 such events have been found. The asymmetry parameter is defined by

$$A_{\tau'} = \frac{(N^+ - N^-)}{\frac{1}{2}(N^+ + N^-)}$$

where N^{\pm} are the numbers of K^{\pm} decaying by the τ' mode normalised to the number of $K^{\pm} \rightarrow \pi^{\pm} \pi^0$ decays. The distribution of values of $A_{\tau'}$ for 49 independent samples of data is shown in figure 36. The values follow a Gaussian distribution, with a mean of -0.0009 ± 0.0055 . This result is consistent with zero.

These events have also been used to determine the asymmetry of the slope parameter a in the τ' decay matrix element $M \propto (1+aY)$ where $Y = (2T_3 - Q)/Q$, T_3 is the kinetic energy of the charged pion and Q is the energy release in the decay. A value of

$$a_{\tau'} = (a_{\tau'^+} - a_{\tau'^-}) / \frac{1}{2}(a_{\tau'^+} + a_{\tau'^-}) = +0.009 \pm 0.008$$

has been obtained. About 800 events of the type $K^{\pm} \rightarrow \pi^{\pm} \pi^0 \gamma$ have been found. This represents about 25% of the total amount of data for this decay mode. For the asymmetry in this decay mode a value of $A_{\pi\pi\gamma} = -0.11 \pm 0.10$ has been obtained.

The conclusion to be drawn from the data analysed so far is that there is no significant evidence for a violation of CP invariance in either decay mode.

Experiment 15

UNIVERSITY OF CAMBRIDGE
RUTHERFORD LABORATORY

Investigation of
Bremsstrahlung
Anomalies

When a light charged particle passes close to an atomic nucleus it is accelerated by the electric force between the two and as a result of this acceleration it is deflected from its original path and loses some of its energy in the form of a γ -ray (bremsstrahlung - braking radiation). The distribution of fractional energy losses in such processes can be calculated accurately using quantum electrodynamic theory. Such calculations indicate a smoothly decreasing probability as the radiated energy increases. Some recent bubble chamber results (described in the 1969 Annual Report) have indicated that a supposedly pure electron beam did not behave in this predicted way or, alternatively, that some previously undiscussed light particle existed in the electron beam.

The present experiment consisted of two parts. In the first a very sensitive gas Cerenkov counter was used to analyse the velocities, and hence the masses, of the particles in a beam of fixed momentum. In such an investigation the counting rate of the Cerenkov counter is recorded as the pressure of the gas inside it is increased. Such a curve is shown in figure 37. Any new particle heavier than the electron would show as a sharp step in the counting rate on the otherwise flat portion of the curve; a particle lighter than the electron would be detected below the electron threshold. No such effects were observed. Departures from the pressure curves for electrons are plotted in figure 38, from which it is concluded that there is no evidence for any new particle with a mass below $45 \text{ MeV}/c^2$.

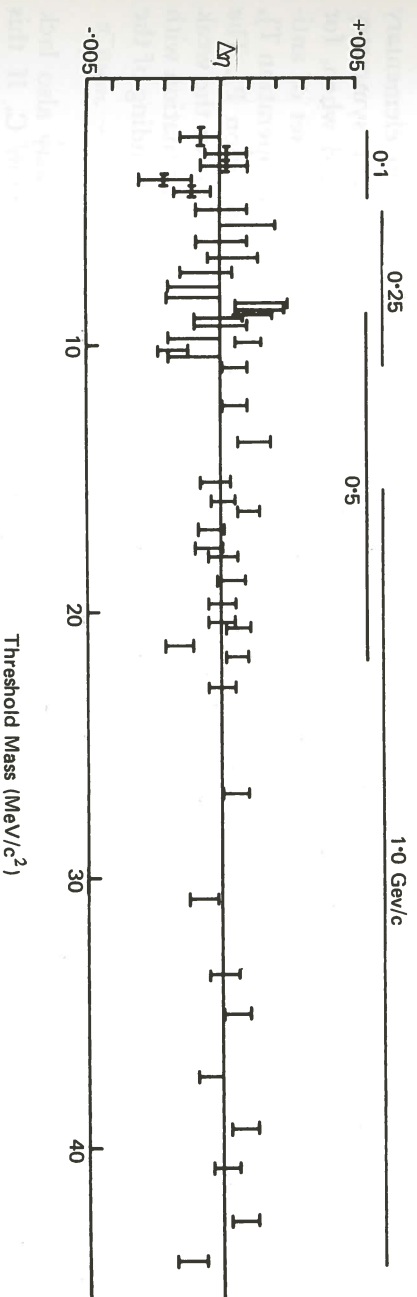


Figure 38. Measured departures from the expected gas Cerenkov counter pressure curves for electrons plotted against the threshold mass of the hypothetical particle. Horizontal lines at top of figure indicate mass regions covered by given electron beam momentum.